Process Safety and Environmental Protection 207 (2026) 108352

Contents lists available at ScienceDirect

Process Safety and Environmental Protection

journal homepage: www.journals.elsevier.com/process-safety-and-environmental-protection

Ex-ante assessment of life cycle inherent safety (ExALIS) of industrial value chains

Federica Tamburini, Lorenzo Pasquali, Alessandro Dal Pozzo, Alessandro Tugnoli, Valerio Cozzani *

LISES – Laboratory of Industrial Safety and Environmental Sustainability, Department of Civil, Chemical, Environmental, and Materials Engineering, University of Bologna, via Terracini n.28, Bologna 40131, Italy

ARTICLE INFO

Keywords:
inherent safety
consequence analysis
value chain
life cycle assessment
early design
failure frequency database

ABSTRACT

A holistic life cycle assessment of industrial value chains requires integrating the prospective safety performance of technologies, to reduce or eliminate potential impacts of accidents on humans and the environment. This study introduces a novel consequence-based inherent safety methodology—ExALIS (Ex-ante Assessment of Life cycle Inherent Safety)—designed to support proactive hazard identification during the conceptual design phase of industrial value chains. Unlike conventional approaches that focus on single process units, ExALIS adopts a life cycle perspective, addressing safety-related concerns across the entire value chain. By integrating inherent safety principles with life cycle analysis, it provides a holistic assessment, highlighting the impact of technological decisions on human health and the environment. Its modular design ensures adaptability across diverse sectors and decision-making contexts. To demonstrate its capabilities, ExALIS was applied to a case study addressing technological alternatives (biomethane and hydrogen) for clean energy supply to ceramic manufacturing plants. The findings show that ExALIS is able to assess latent hazards in seemingly sustainable options, highlighting the critical importance of an early incorporation of safety considerations in the design process to support forward-

Abbreviations: A, Asset; AIRI, Anticipated Inherent Risk Index; BioM, Biomethane; BLEVE, Boiling Liquid Expanding Vapor Explosion; C&EI, Dow Chemical and Exposure Index; CH_4, Methane; CISI, Comprehensive Inherent Safety Index; CO_2, Carbon Dioxide; D, Diameter; E, Environment; EHS, Environmental, Health, and Safety Index; EISI, Extended Inherent Safety Index; ExALIS, Ex-ante Assessment of Life cycle Inherent Safety; F&EI, Dow Fire and Explosion Index; G, General; GISAT, Graphical Inherent Safety Assessment Technique; GRAND, Graphical Descriptive Technique for Inherent Safety Assessment; H, Human; H_2, Hydrogen; H_2O, Water; H_2S, Hydrogen Sulfide; HI, Hazard Indicator; HIRA-FEDI, Hazard Identification and Ranking -Fire and Explosion Damage Index; I2SI, Integrated Inherent Safety Index; IBI, Inherent Benign-ness Indicator; ICPRI, Inherent Chemical Process Route Index; IDLH, Immediately Dangerous to Life and Health concentration; INSET, INherent SHE Evaluation Tool; IPI, Inherent Process Index; IRDI, Inherent Risk Design Index; I-Safe, i-Safe Index; ISAPEDS, Inherent Safety Assessment Technique for Preliminary Design Stage; ISI, Inherent Safety Index; ISIM, Inherent Safety Index Module; IS-KPI, Inherent Safety Key Performance Indicator; KOH, Potassium Hydroxide; KPI, Key Performance Indicator; LCA, Life Cycle Assessment; LFL, Lower Flammability Limit; LOC, Loss Of Containment; MIMAH, Methodology for Identifying Major Accident Hazards; Mond FETI, Mond Fire, Explosion and Toxicity Index; N, Node; NaOH, Sodium Hydroxide; NBP, Normal Boiling Point; NFHIH, Node Flammability inherent Hazard index for Human target; NHIA, Node inherent Hazard index for Asset target; NHIE, Node inherent Hazard index for Environment target; NHIH, Node inherent Hazard index for Human target; NOHIH, Node Overpressure inherent Hazard index for Human target; NPIA, Node Potential hazard index for Asset target; NPIE, Node Potential hazard index for Environment target; NPIH, Node Potential hazard index for Human target; NTHIH, Node Toxicity inherent Hazard index for Human target; NuDIST, Numerical Descriptive Inherent Safety Technique; O_2, Oxygen; P, Pipe-like; PFD, Process Flow Diagram; PI, Potential Indicator; PIIS, Prototype Index of Inherent Safety; PNEC, Predicted No Effect Concentration; PRI, Process Risk Index; PSI, Process Stream Index; RC, Release Class; RISI, Risk-based Inherent Safety Index; RM, Release Mode; S, System; SHIA, System inherent Hazard index for Asset target; SHIE, System inherent Hazard index for Environment target; SHIH, System inherent Hazard index for Human target; SPIA, System Potential hazard index for Asset target; SPIE, System Potential hazard index for Environment target; SPIH, System Potential hazard index for Human target; SSbD, Safe and Sustainable by Design; SSI, Stream Safety Index; SWeHI, Safety Weighted Hazard Index; T, Tank-like; TH, Total Holdup; TORCAT, Toxic Release Consequence Analysis Tool; TRL, Technology Readiness Level; U, Unit; UFHIH, Unit Flammability inherent Hazard index for Human target; UHIA, Unit inherent Hazard index for Asset target; UHIE, Unit inherent Hazard index for Environment target; UHIH, Unit inherent Hazard index for Human target; UOHIH, Unit Overpressure inherent Hazard index for Human target; UPIA, Unit Potential hazard index for Asset target; UPIE, Unit Potential hazard index for Environment target; UPIH, Unit Potential hazard index for Human target; UTHIH, Unit Toxicity inherent Hazard index for Human target; VCE, Vapor Cloud Explosion; WISI, Weighted Inherent Safety Index.

* Corresponding author.
E-mail address: valerio.cozzani@unibo.it (V. Cozzani).

https://doi.org/10.1016/j.psep.2025.108352
Received 22 October 2025; Received in revised form 7 December 2025; Accepted 20 December 2025
Available online 22 December 2025

looking design strategies. Overall, ExALIS offers a practical and systemic tool to support the design of safer, cleaner, and more resilient industrial processes.

Nomenclature

c_{f_y}	Credit factor (y^{-1})
$\bar{f}_{u,s}$	Utilization fraction vector composed of M $f_{u,s,m}$
$\bar{p}_{u,s,m}$	Vector collecting the production capacity of a unit and all the input flowrates required by that unit from other units of the system
$h_{s,m,k,i}$	Damage vector for human target
$A_{s,m,k,i}$	Damage vector for asset target
$B_{s,m,k,i}$	Damage vector for environment target
$F_{w,k}$	Mass flow rate of inlet stream w in node k
L_v	Length of a single trip
$c_{f_{y_{eff}}}$	Effective credit factor (y^{-1})
c_{f_i}	Credit factor associated with LOC i
$c_{f_{km}}$	Credit factor for unit length ($y^{-1}km^{-1}$)
$d^{calc}_{s,m,k,i,g,j}$	Damage distance for human target calculated with the consequence model
$d^{eff}_{s,m,k,i,g,j}$	Effective damage distance for human target used for the calculation of the KPIs
$f_{s,m,k,i}$	Flammable damage vector for human target
f_u	Utilization fraction
$o_{s,m,k,i}$	Overpressure damage vector for human target
$\bar{p}$	Vector containing the production capacity of the system (P) and zeros for all other flowrates within the system
p_u	Production capacity of a unit
$t_{s,m,k,i}$	Toxic damage vector for human target
v_m	Mean velocity
τ_B	Effective usage time
τ_v	Mean trip time
τ_y	Number of hours in a year (8766 h/y)
C	Transport capacity
K	Progressive integer referring to the total number of nodes of the unit
M	Progressive integer referring to the total number of units of the system
P	Overall production capacity
W	Progressive integer referring to the total number of inlet streams
g	Progressive integer referring to the release mode
i	Progressive integer referring to the loss of containment event
j	Progressive integer referring to the end-point scenario
k	Progressive integer referring to the node of the unit
m	Progressive integer referring to the unit of the system
n	Total number of trips per year
s	Progressive integer referring to the system
w	Progressive integer referring to the inlet stream
σ	Corrective factor

1. Introduction

The early assessment of safety issues in the design of manufacturing processes and value chains is a critical factor to ensure a sustainable and responsible industrial development (Park et al., 2020; Qian et al., 2024). A clear and compelling call for the adoption of a life-cycle perspective, merging safety and environmental impacts, is growing worldwide, as documented, e.g., by the recent "*Safe and sustainable by design*" (SSbD) framework proposed by the European Commission (Abbate et al., 2024; Caldeira et al., 2022b, 2022a).

As industries increasingly adopt innovative technologies and complex value chains, the proactive identification and mitigation of potential hazards becomes crucial (Hendershot, 1997; Pu et al., 2023). A delay in recognizing inherent hazards can lead to costly design modifications, operational inefficiencies, and increased risks for human health and the environment (Khan and Amyotte, 2004). Additionally, late-stage safety interventions often require significant financial and logistical efforts, making early safety assessments not only a technical necessity but also a strategic advantage. By incorporating safety considerations at the inception of process design, industries can enhance resilience, ensure regulatory compliance, and improve long-term operational efficiency.

Consequently, integrating safety assessments at the initial stages of process design is paramount to achieve inherently safer and more sustainable industrial systems, fostering both economic and environmental benefits (CCPS, 2019; Hendershot, 2006; Khan et al., 2003; Park et al., 2020). A similar advantage has been widely recognized in the environmental domain, where numerous studies have shown that considering prospective environmental impacts during early-stage process design, i.e., through the *ex-ante* application of quantitative sustainability assessment (Cucurachi et al., 2018), can significantly improve the environmental performance of novel processes and emerging technologies (Bergerson et al., 2020). By anticipating potential environmental hotspots and trade-offs, *ex-ante* life cycle assessment (LCA) enables designers and decision-makers to steer technological development toward more sustainable configurations before key design choices become locked in (Arvidsson et al., 2017; Buyle et al., 2020; Thonemann et al., 2020). Extending this forward-looking perspective to process safety further ensures that also potential accident-related impacts, which are not in principle correlated to expected impacts from routine operation are properly taken into account (Zanobetti et al., 2025).

Inherent safety, a well-established concept in process safety engineering, aims to eliminate or significantly reduce hazards rather than to manage them through add-on safety measures (Kletz, 1996; Kletz and Amyotte, 2010). It is built upon key principles such as minimization, substitution, moderation, and simplification, which collectively contribute to reducing the likelihood and severity of accidents (Mannan, 2012). Previous literature, stemming from both academic research and industrial initiatives, has extensively addressed inherent safety assessment methods, primarily focusing on specific plant-level processes (Crivellari et al., 2021a; Gao et al., 2021; Janošovský et al., 2022; Kidam et al., 2016; Roy et al., 2016; Tamburini et al., 2025b, 2024b; Tugnoli et al., 2007). Examples of these traditional approaches are the Dow Fire and Explosion Index (F&EI) (Gupta et al., 2003), the Dow Chemical and Exposure Index (C&EI) (AIChE technical manual, 1998), the Inherent Safety Index (ISI) (Rahman et al., 2005), the Risk-based Inherent Safety Index (RISI) for evaluating alternative designs (Rathnayaka et al., 2014), and the Process Risk Index (PRI) (Chau et al., 2022). These tools typically rely on material properties, process parameters, and empirical data to quantify risk within a predefined boundary. While effective for identifying specific process-related hazards, they often fall short in capturing the broader dynamics of modern industrial systems. A key limitation of these methods is their inability to account for

interdependencies across unit operations, supply chains, and external environmental influences—factors that can give rise to cascading or systemic risks. Additionally, many indices operate independently of well-established environmental and sustainability assessment frameworks, such as life cycle assessment (LCA) (Ee et al., 2020; Tamburini et al., 2025a). For example, while the F&EI (Gupta et al., 2003) and C&EI (AIChE technical manual, 1998) effectively address specific operational hazards, they do not consider the full environmental footprint or sustainability of a product or process across its life cycle (AIChE technical manual, 1998; Gupta et al., 2003). As industry evolves toward integrated and complex systems, these limitations become increasingly critical. There is a growing need for comprehensive inherent safety assessment frameworks that move beyond the assessment of individual units or operations, offering an integrated understanding of safety and risks associated to an entire value chain. This avoids focusing on the local safety optimization of a single process step, potentially shifting hazards toward upstream and/or downstream operations. Such need is underscored by the expanding range of applications in which inherent safety plays a central role (Gao et al., 2021), including the nuclear power industry (Sofu, 2015), offshore facilities (Crivellari et al., 2021a), dust explosion prevention and mitigation (Rathnayaka et al., 2014) and risk-based safety interventions (Khan et al., 2002).

To address this methodological gap, a novel consequence-based inherent safety methodology is proposed, named ExALIS (Ex-ante Assessment of Life cycle Inherent Safety). The method is designed to assess inherent safety within an integrated, life cycle context. The proposed framework includes the following elements of novelty:

i) It enables an ex-ante application of inherent safety principles during the early conceptual design phase of industrial projects, allowing for proactive hazard identification and mitigation. This early-stage integration supports the minimization of risk at the outset, reducing the need for costly retrofitting or late-stage risk management interventions.
ii) It expands the scope of inherent safety assessment beyond individual equipment items, plants or core processes, to encompass the entire value chain, ensuring a more comprehensive evaluation of safety implications. This holistic approach allows industries to identify interdependencies and potential risk propagation across different stages of the value chain, leading to more informed and effective decision-making.
iii) Offering integrability and modularity with environmental LCA, it facilitates a systematic analysis of trade-offs, in particular those potentially arising between safety and environmental sustainability aspects. By integrating safety assessment with environmental impact evaluation, ExALIS provides a multi-dimensional framework that supports balanced decision-making in sustainable process development.

Bridging the gap between inherent safety assessment and life cycle thinking, ExALIS provides a robust and scalable approach to the improvement of safety performance in industrial systems. The methodology fosters informed decision-making at the early design stages, contributing to the development of inherently safer, more sustainable, and economically viable industrial processes. Furthermore, its adaptability allows for seamless integration into existing design workflows, making it a practical tool for industries aiming to enhance both safety and sustainability in their operations.

In the following, Section 2 provides a comprehensive review of the literature on the inherent safety approaches developed to date and Section 3 presents and describes the methodology designed to quantitively assess the inherent safety of entire value chains through the evaluation of key hazard indices. Section 4 applies this methodology to a comparative case study involving two alternative technological pathways—biomethane and hydrogen production—for decarbonizing the ceramic sector. Section 5 provides an extensive discussion of the obtained results, and Section 6 draws some conclusions.

2. State of the art in inherent safety assessment

Over the past three decades, a broad spectrum of inherent safety assessment tools has emerged to systematically compare process alternatives and support the selection of inherently safer options (Park et al., 2020). These methods can be clustered in five main categories: i) parameter-based indexing methods; ii) consequence-based evaluation methodologies; iii) graphical approaches; iv) integrated safety–environment evaluation; and v) risk-based methods (Zanobetti et al., 2023). A chronological collection of these approaches is provided in Table 1 with the respective categories.

The first group of methodologies comprises parameter-based approaches which quantify inherent safety by scoring process- and substance-related attributes through weighted contributions from chemical hazards, operating conditions, and equipment characteristics. Early system-level methods, such as the Prototype Index of Inherent Safety (PIIS) (Lawrence, 1996) and later the Inherent Safety Index (ISI) (Rahman et al., 2005), played a pivotal role in establishing a structured comparison of alternative process routes. Although PIIS was among the first to consider entire production routes rather than individual units, its semi-quantitative structure does not fully capture the interdependencies among process stages or the propagation of hazards along the value chain. More recent system-level indices, such as the novel indexes proposed by the ExALIS methodology in the present study, extend this conceptual space by quantitatively linking hazards across interconnected units using unified indicators and flow-based aggregation rules, enabling life-cycle interpretations, the consistent treatment of multi-unit systems, and the integration with environmental assessment frameworks.

The second category of methodologies includes consequence-based methods which evaluate inherent safety by analysing the outcomes of fires, explosions, and toxic releases. Classical indices such as the Dow Fire and Explosion Index (F&EI) (Gupta et al., 2003) and the Dow Chemical Exposure Index (C&EI) (AIChE technical manual, 1998), together with later developments as the Integrated Inherent Safety Index (I2SI) (Khan and Amyotte, 2004) and the subsequent contributions by Tugnoli et al. (Tugnoli et al., 2007), incorporate increasingly refined consequence modelling. These approaches have been widely applied across domains including hydrogen storage, biogas upgrading, biodiesel production, and LNG bunkering, where they support the comparison of design alternatives considering credible accident scenarios.

A third methodological family comprises graphical approaches, which often serve as intuitive extensions of parameter-based indices. Tools such as the Process Risk Index (PRI) (Chau et al., 2022), the Process Stream Index (PSI) (Shariff et al., 2012), and related graphical techniques (Ahmad et al., 2019, 2016) enable visual inspection of hazard contributions and safe operating envelopes. Their visual structure enhances interpretability and fosters communication among engineers and decision-makers during early-stage design.

Beyond strictly safety-oriented metrics, an additional set of tools incorporates environmental and occupational health dimensions alongside inherent safety principles. Indices such as the Inherent Benignness Indicator (IBI) (Srinivasan and Trong, 2008) and the Inherent Chemical Process Route Index (ICPRI) (Warnasooriya and Gunasekera, 2016) employ multivariate parameter sets to capture environmental burdens, toxicological properties, and process hazards simultaneously. These methods broaden the scope of inherent safety assessment toward integrated sustainability considerations.

A final category comprises risk-based approaches, which combine consequence and likelihood into a unified representation of inherent risk. Methods such as the Risk-Based Inherent Safety Index (RISI) (Rathnayaka et al., 2014) contrast baseline design risks with the reduced risks achievable through inherently safer alternatives. By embedding probabilistic information, these frameworks offer a more nuanced

Table 1
Collection of inherent safety approaches available in the literature per category.

INHERENT SAFETY INDEX	ACRONYM	CATEGORY	REFERENCE
Mond Fire, Explosion and Toxicity Index	Mond FETI	Consequence-based	(Doran and Greig, 1993)
Prototype Index of Inherent Safety	PIIS	Parameter-based	(Lawrence, 1996)
INherent SHE Evaluation Tool	INSET	Graphical method	(Mansfield et al., 1997)
Hazard Identification and Ranking -Fire and Explosion Damage Index	HIRA-FEDI	Consequence-based	(Khan and Abbasi, 1998)
Dow Chemical Exposure Index	C&EI	Consequence-based	(AIChE technical manual, 1998)
Inherent Safety Index	ISI	Parameter-based	(Heikkil, 1999)
Environmental, Health, and Safety Index	EHS	Safety-environment	(Koller et al., 2000)
Safety Weighted Hazard Index	SWeHI	Parameter-based	(Khan et al., 2001)
i-Safe Index	i-Safe	Parameter-based	(Palaniappan et al., 2002b, 2002a)
Dow Fire and Explosion Index	F&EI	Consequence-based	(Gupta et al., 2003)
Integrated Inherent Safety Index	I2SI	Consequence-based	(Khan and Amyotte, 2004)
Inherent Safety Key Performance Indicator	IS-KPI	Consequence-based	(Tugnoli et al., 2007)
Inherent Safety Index Module	ISIM	Graphical method	(Leong and Shariff, 2008)
Inherent Benign-ness Indicator	IBI	Safety-environment	(Srinivasan and Trong, 2008)
Toxic Release Consequence Analysis Tool	TORCAT	Consequence-based	(Shariff and Zaini, 2010)
Extended Inherent Safety Index	EISI	Parameter-based	(Li et al., 2011)
Process Stream Index	PSI	Graphical method	(Shariff et al., 2012)
Comprehensive Inherent Safety Index	CISI	Parameter-based	(Gangadharan et al., 2013)
Inherent Risk Design Index	IRDI	Parameter-/risk-based	(Rusli et al., 2013)
Risk-based Inherent Safety Index	RISI	Risk-based	(Rathnayaka et al., 2014)
Numerical Descriptive Inherent Safety Technique	NuDIST	Consequence-based	(Ahmad et al., 2014)
Inherent Process Index	IPI	Parameter-based	(Jiao and Xiang, 2016)
Inherent Chemical Process Route Index	ICPRI	Safety-environment	(Warnasooriya and Gunasekera, 2016)
Graphical Descriptive Technique for Inherent Safety Assessment	GRAND	Graphical method	(Ahmad et al., 2016)
Inherent Safety Assessment Technique for Preliminary Design Stage	ISAPEDS	Consequence-based	(Ahmad et al., 2017)
Graphical Inherent Safety Assessment Technique	GISAT	Graphical method	(Ahmad et al., 2019)
Process Risk Index	PRI	Graphical method	(Chau et al., 2022)
Weighted Inherent Safety Index	WISI	Parameter-based	(Bassani et al., 2023)
Anticipated Inherent Risk Index	AIRI	Risk-based	(Norouzi et al., 2024)
Stream Safety Index	SSI	Risk-based	(Pelucchi et al., 2025)

representation of the trade-offs between hazard elimination, substitution, attenuation, and the reduction of event frequencies.

3. Methodology

The ExALIS methodology consists of a consequence-based inherent safety approach developed to comprehensively model value chains and production processes. As shown in Fig. 1, it is structured into eight steps, which are described in detail below. A template supporting the implementation of the methodology is freely available on request at https://site.unibo.it/lises/en/research-fields/ex-alis or may be requested at the following e-mail address: dicam.lises.exalis@unibo.it

3.1. Step 1: definition of the goal and scope of the analysis

3.1.1. Goal and scope of the analysis

The proposed methodology is intended as a decision-support tool for the preliminary inherent safety assessment of processes and value chains for chemical products and energy vectors. It is conceived to allow its application at any stage of the process lifecycle since the early stages of development (conceptual design). Thus, it allows as well the assessment of value chains and systems at low technology readiness levels (TRLs).

The value chain, defined as the collection of the steps required to create a given final product, constitutes the system to be studied. Value chain concept extends beyond the classical concept of chemical process route, as it accounts also for operations such as storage, transportation and auxiliary systems that are needed for the actual implementation of a process route in the real word. When alternative value chains or different embodiments of the same value chain exist to generate the same product, a comparative study can be of concern: this will address the assessment of a number of alternative systems, one for each option to

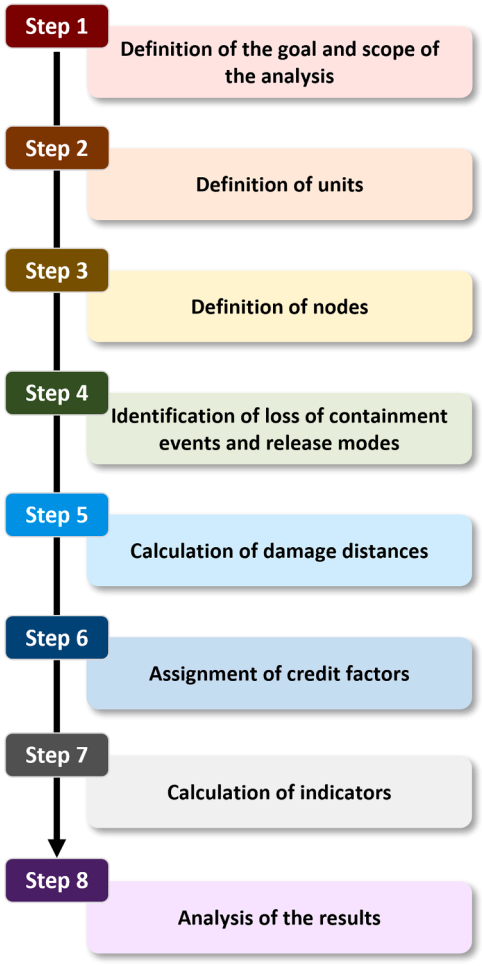

Fig. 1. Flowchart of the ExALIS methodology.

be considered within the scope of the analysis.

Given the diverse objectives and circumstances of each study, the first step of the methodology is to define the goal and scope of the analysis based on its intended application. Stating the goal of the analysis consists in defining the system that will be analyzed, its boundaries and the purpose for conducting an inherent safety assessment, i.e., the specific questions that the assessment is meant to answer. In the execution of comparative assessments, particular care should be taken in the definition of a representative production capacity of the system (see Section 3.1.4). Alternatively, or in addition to comparative assessments, the analysis might be intended to identify the most critical components of a system (units and nodes, as defined in Section 3.1.3) or the most critical end-point scenarios (as defined in Section 3.5.1), in order to provide guidance for the following steps of process design. Finally, the scope shall define, according to the goal, the key performance indicators (KPIs) to be used in the assessment among the ones presented in Section 3.7.

3.1.2. Definition of the system

In the present context, a system is a collection of processes (units) that constitute an embodiment of the value chain of a chemical product. In case of comparative assessments, all the systems shall have the same production capacity for the chemical of concern. In the conceptual design phase, inherent safety considerations are addressed by adapting the depth and rigor of the analysis to the level of detail of the available information. Typically, this includes preliminary process flow diagrams (PFDs), preliminary mass and energy balances, and initial assumptions regarding operating conditions. Even if the process is only partially defined, these baseline data enable a first screening of inherent safety aspects, which are then iteratively expanded and validated as the design progresses and more detailed data become available.

System boundaries define what shall be included or excluded in the study: in particular all the units that are part of the value chain of concern and that handle hazardous materials shall be included in the system boundaries. The selection of system boundaries shall use consistent criteria among systems in comparative studies in order to avoid distortions in the results (e.g., production of electrical power, thermal power and catalysts shall be consistently excluded from boundaries in all alternative systems).

3.1.3. System breakdown to units and nodes

In the analysis, it is functional to break down a system into units. In turn, each unit shall be divided into nodes. A unit is a specific step in the value chain of the product, such as the extraction of raw materials, any production or transformation process, transportation, and utilization. A node is the smallest element considered in the analysis for which information on the process conditions and/or input and output material flows are collected (e.g., an equipment). For relatively simple processes, unit and node might coincide. Fig. 2 schematizes the relationships between units and nodes within a system. Clearly enough, the minimum configuration for the analysis is a system composed by a single unit in turn composed of a single node.

3.1.4. Production capacity and utilization factors

The production capacity P of the system is the yearly amount of final product to which the quantitative results of the analysis, i.e., the quantified values of the KPIs, are referred. In other words, it is the reference unit of the analysis and can be quantified in terms of mass or energy, according to the intended application of the study. The concept is analogous to the definition of functional unit in environmental LCA studies (ISO, 2020a, 2020b).

For the comparative assessment of alternatives systems or value chains producing the same chemical product, the comparison is typically carried out considering the same production capacity, expressed in terms of the mass of product generated yearly by each system. However, when comparing systems that produce different energy vectors, a mass-based comparison is not meaningful, as different vectors deliver varying amounts of energy per unit mass depending on their heating values and on the efficiencies of their respective energy conversion processes. In such cases, the production capacity shall be expressed in terms of the yearly energy available for final use.

Each unit in the system presents its own production capacity p_u (see Fig. 2), which may relate to the final product or to precursors, reactants, intermediates, solvents, auxiliary materials required for its production, depending on the role of the unit within the system. The definition of a utilization factor may be required to correctly account for the share of utilization of units and nodes that contribute to the production capacity of the final product. If the entire output of all units and nodes in the system is finalized to obtain the final product, it is straightforward to associate the inherent hazards of all units and nodes with the production capacity, P, of the system. Conversely, when only a fraction of a unit

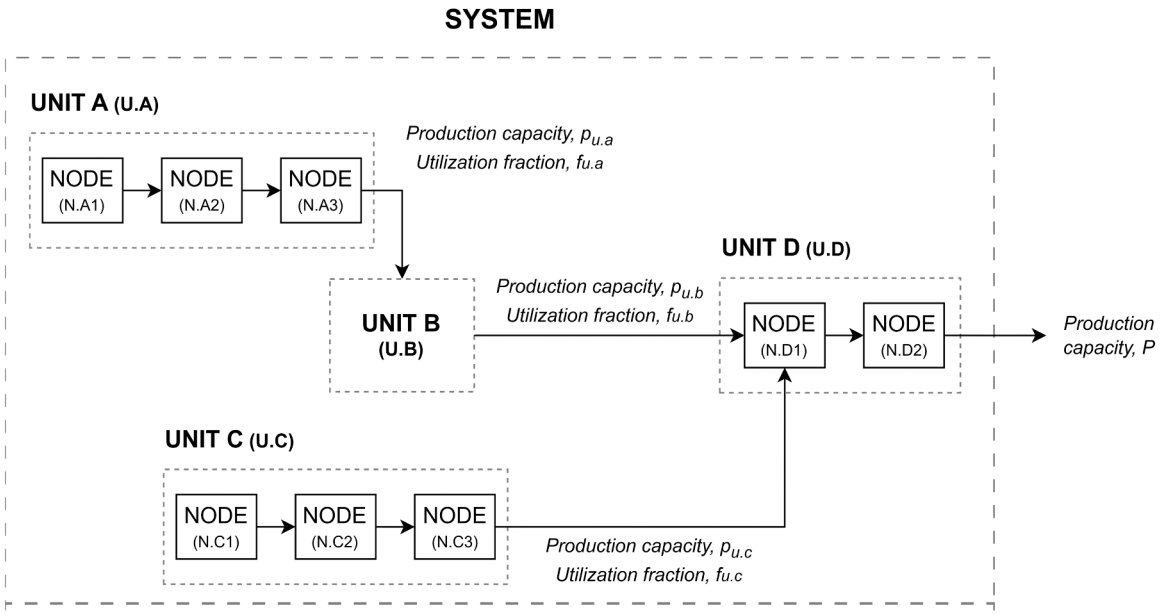

Fig. 2. Example of a system representation by units and nodes.

production is dedicated to the system of interest, a utilization fraction, f_u (see Fig. 2), shall be defined.

Let $\overline{p}_{u,s,m}$ be the vector collecting the production capacity of a unit and all the input flowrates (expressed as yearly flowrates) required by that unit from other units of the system (negative values for inputs and positive for production capacity). The matrix A_s, whose columns are all the $\overline{p}_{u,s,m}$ vectors for the M units of the s^{th} system, is used to calculate the utilization factor vector $\overline{f}_{u,s}$ as follows:

$$\overline{f}_{u,s} = {A_s}^{-1} \bullet \overline{p} \quad (1)$$

where ${A_s}^{-1}$ is the inverse of matrix A_s, and $\overline{p}$ is a vector that contains the production capacity of the system (P) and zeros for all other flowrates within the system. The utilization factors, $f_{u,s,m}$, are the M elements of $\overline{f}_{u,s}$. This approach is analogous to the matrix scaling used in LCA for the quantification of the lifecycle inventory (European Commission - JRC, 2010). Specific rules apply when calculating system KPIs in the presence of utilization factors, discussed in Section 3.7.

When a unit produces multiple useful products but only some are relevant to the system, an allocation need arises. This can be managed defining allocation factors by the consolidated approaches used in LCA studies (European Commission - JRC, 2010; ISO, 2020b). The allocation factors are to be used similarly to utilization factors in the definition of the inherent safety KPIs.

3.1.5. Selection of key performance indicators (KPIs)

The selection of the key performance indicators (KPIs) to be used in the inherent safety assessment is made according to the intended application of the study.

Two types of inherent safety KPIs are adopted:

- Potential Indicator (PI): quantifies the magnitude of the worst-case scenario affecting the node, unit, or system under study;
- Hazard Indicator (HI): quantifies the inherent hazard associated to each credible scenario affecting the node, unit, or system under study, considering both the magnitude and the credibility of the potential consequences.

The indicators can be calculated at the node (N), unit (U), and system (S) level according to the rules of calculation described in Section 3.7, and are defined with reference to the three possible targets of an accident: human (H), asset (A), and the environment (E). KPIs for different targets may be defined, requiring the definition of an appropriate damage and a related threshold value, as outlined in Section 3.5.2.

According to the aim of the assessment, all or part of the KPIs listed in Table 2 can be used.

3.2. Step 2: definition of units

Once the goal and scope of the analysis are defined, the second step of the methodology involves defining units.

A system represents a potential embodiment of the value chain for a product or its components, comprising multiple units and nodes, as previously illustrated in Fig. 2. When evaluating a single step of the value chain, the system aligns with the corresponding unit.

A system reference scheme must be defined for each system assessed in Step 1. Reference schemes must then be defined for all the constituent units, which serve distinct functions such as production (e.g., process plants), storage (e.g., temporary depots), distribution (e.g., refueling stations), transportation (e.g., pipelines, road tankers), or transfer (e.g., loading/unloading arms and pumping stations). The reference schemes shall include simplified PFDs or equivalent technical representations, such as schematics for transport tankers, ensuring that the necessary information for each unit is captured. An example is provided for the case study described in Section 3.

One or more nodes shall be associated to each unit. The features and the function of nodes is described in the following section.

For each unit, the input and output flowrates of the streams exchanged with other units of the system shall be calculated. These allow the definition of the vector $\overline{p}_{u,s,m}$ defined in Section 3.1.4. It shall be noted that data on material/energy flows exchanged with items that are not part of the system are not necessary for the calculation.

3.3. Step 3: definition of nodes

To finalize the definition of the constituting elements of a system, the third step of the methodology entails the identification of the nodes. Nodes represent the individual components within each unit of the system, and can include process equipment (e.g., columns, heat exchangers, and reactors), transport equipment (e.g., pipelines and tankers), or transfer equipment (e.g., hoses and arms).

Nodes are classified into four macro-categories:

1. Process Nodes (all-purpose): encompass all major process units applicable across various types of plants.
2. Process Nodes (specialized): include equipment specific to particular industrial sectors, such as Oil&Gas, hydrogen, and others.
3. Transport Nodes: comprise equipment used for fluid transportation between plants, including pipelines, ship, and road and rail tankers.
4. Transfer Nodes: includes hoses and transfer arms used for fluid transfer operations.

Nodes that involve hazardous substances or substances stored under hazardous conditions must be identified and further categorized into three equipment classes, based on the relative importance of inventory and input streams on the definition of release severity:

- General (G), where a check, described in Table 4, is required to determine if either the equipment inventory or the inlet streams dominate the release severity;
- Tank-like (T), where the equipment inventory determines the release severity;
- Pipe-like (P), where the inlet streams determine the release severity.

Table 2
Nomenclature of the KPIs proposed by the methodology (H: Human; A: Asset; E: Environment).

GROUP	KPIs			ASSESSMENT
	NODE	UNIT	SYSTEM	
H	NPIH, NHIH	UPIH, UHIH	SPIH, SHIH	Inherent safety related to the human target
A	NPIA, NHIA	UPIA, UHIA	SPIA, SHIA	Inherent safety related to the asset target
E	NPIE, NHIE	UPIE, UHIE	SPIE, SHIE	Inherent safety related to the environmental target

Table 3
Information required for each node, depending on the related equipment class.

INFORMATION	EQUIPMENT CLASS		
	GENERAL	TANK-LIKE	PIPE-LIKE
Nominal temperature and pressure of the equipment	✓	✓	
Nominal temperature and pressure of inlet/outlet streams	✓		✓
Composition, flow rate of inlet/outlet streams	✓		✓
Physical state of inlet/outlet streams	✓		✓
Inventory, composition and physical state	✓	✓	
Pressure or liquid head (only for atmospheric equipment)	✓	✓	

Table 4
Sub-classes of the general class of equipment ($F_{w,k}$: mass flow rate of inlet stream w in node k; W: total number of inlet streams).

CLASS	SUB-CLASS	CRITERION
GENERAL	G_T	$TH_k > \sum_{w=1}^{W} F_{w,k} \bullet 3$ min
	G_P	$TH_k < \sum_{w=1}^{W} F_{w,k} \bullet 3$ min

Depending on the equipment class to which the node belongs, specific information is required to complete the inherent safety assessment, as summarized in Table 3.

Nodes that do not involve the presence of hazardous substances can be neglected in the further steps of the analysis, unless specific hazard scenarios leading to end-point scenarios similar to those accounted in Step 5 can be identified (e.g., physical explosion of a pressurized inert gas vessel).

It is important to note that in Table 3, the term "inventory" generally refers to the total mass of fluids contained within the equipment under operating conditions, commonly also indicated as the total holdup (TH). If the inventory fluctuates during normal operations (e.g., in storage tanks), the highest expected value is considered as the inventory. If the gas phase has hazard characteristics similar or less severe than the liquid phase, gas inventory can be neglected.

Within the general class of equipment, two sub-classes—G_T and G_P—are defined based on whether the inventory or the inlet streams have a greater influence on release severity, respectively. This distinction is further clarified in Table 4, which outlines the criteria to determine which element prevails. In the table, k is the tag of the node of interest, $F_{w,k}$ represents the mass flow rate of the inlet stream w entering node k, and W indicates the total number of inlet streams.

Table 5, Table 6, Table 7, and Table 8 summarize the taxonomy of process, transport, and transfer nodes.

3.3.1. Additional information for transport units, transfer units, and batch processes

Dealing with transport and transfer units, as well as with batch processes, requires additional information in order to conduct the inherent safety assessment.

Focusing on the transport units, if pipelines are involved, details about the length of the pipeline and the number of pumping stations for each pipeline are necessary. For rail, road, and maritime tankers, the length of a single trip (L_v) and the mean velocity of the vehicle (v_m) are required for the evaluation.

Special considerations apply when defining nodes in pipeline transport units. A distinct node is defined for each segment of the pipeline having a constant nominal diameter, regardless of the number of pumping stations present. Each piece of equipment in pumping stations is considered as an individual node, similarly to what occurs for process units. If multiple pumping stations are present, multiple nodes are therefore considered accordingly in the pipeline transport unit under assessment.

In the case of units featuring transportation by rail, road, or maritime tankers, the nodes of the transport unit are the specific types of tankers used in the operation (road, rail, or ship/barge), classified according to their capacity (in kg) and to the physical properties of the delivered fluid in terms of temperature and pressure. As an example, if a transportation unit uses two types of road tankers to deliver a given fluid, at the same pressure and temperature but with different capacities, two distinct nodes shall be considered. However, if tankers have also identical capacities, they are accounted as a single node.

A transfer unit is typically composed of loading/unloading arms and/or hoses and pumping stations where necessary. Each hose or arm is considered as a distinct node within the transfer unit. These units require additional information on the number of transfers per year. The number should coincide with the number of trips considered in the transport units servicing the transfer unit.

In the case of seasonal processes and processes involving batch operations, the additional information required is the effective usage time (τ_B) of each node, which represents the operational time during which the equipment is in service each year.

Table 5
Taxonomy of process nodes (all-purpose) (D: diameter).

PROCESS NODES (ALL-PURPOSE)			
CATEGORY	**SUB-CATEGORY**		**CLASS**
Process vessel	Columns	Atmospheric	G
		Pressurized	G
	Separators	Atmospheric	G
		Pressurized	G
	Filters	Atmospheric	G
		Pressurized	G
	Reactors	Stirred tank	G
		Tubular	P
	Others/Unspecified	Atmospheric	G
		Pressurized	G
Storage tank	Atmospheric		T
	Pressurized		T
	Cryogenic		T
	Tank containers (ISO)		T
Heat exchanger	Shell&Tube		P
	Plate&Frame		P
	Air-coolers		P
	Furnaces/Boilers		P
	Direct Fire Heaters		P
	Others/Unspecified		P
Machinery	Pumps (centrifugal)		P
	Pumps (alternative)		P
	Pumps (others/unspecified)		P
	Compressors (centrifugal)		P
	Compressors (alternative)		P
	Compressors (others/unspecified)		P
	Turbines		P
Piping	Process piping*	$D \leq 6''$	P
		$6'' < D \leq 18''$	P
		$D > 18''$	P
	Permanently installed hoses	$D \leq 6''$	P
		$6'' < D \leq 18''$	P
		$D > 18''$	P
	Temporary hoses	$D \leq 6''$	P
		$6'' < D \leq 18''$	P
		$D > 18''$	P

* this category has to be considered only when the distance between two connected units is higher than 50 m.

Table 6
Taxonomy of process nodes (specialized) (D: diameter).

PROCESS NODES (SPECIALIZED)			
CATEGORY	**SUB-CATEGORY**		**CLASS**
Oil&Gas	Wellhead (surface, subsea)		P
	Pig trap (launcher, receiver)		P
	Manifold, header	$D \leq 6"$	P
		$6'' < D \leq 16''$	P
		$D > 16''$	P
	Riser (steel fixed)	$D \leq 16"$	P
		$D > 16''$	P
	Riser (flexible)	Overall	P
Hydrogen	Fuel cell		G
	Electrolyzer		G
Venting system	Flare/Burner		P
	Venting&Blowdown system		G

3.4. Step 4: identification of loss of containment events and release modes

The fourth step of the methodology involves the identification and characterization of loss of containment (LOC) events leading to end-point scenarios.

Table 7
Taxonomy of transport nodes (D: diameter).

TRANSPORT NODES			
CATEGORY	**SUB-CATEGORY**		**CLASS**
Pipeline	Steel pipeline Offshore	D ≤ 6"	P
		6'' < D ≤ 10''	P
		10'' < D ≤ 16''	P
		D > 16''	P
	Oil pipeline Offshore	D ≤ 6"	P
		6'' < D ≤ 10''	P
		10'' < D ≤ 16''	P
		D > 16''	P
	Gas pipeline Onshore	D ≤ 6"	P
		6'' < D ≤ 10''	P
		10'' < D ≤ 16''	P
		D > 16''	P
Tankers	Road	Atmospheric	T
		Pressurized	T
	Rail	Atmospheric	T
		Pressurized	T
	Ship/Barge	Atmospheric	T
		Pressurized	T

Table 8
Taxonomy of transfer nodes.

TRANSFER NODES			
CATEGORY	**SUB-CATEGORY**		**CLASS**
Loading/Unloading hose	Road	Atmospheric	P
		Pressurized	P
	Rail	Atmospheric	P
		Pressurized	P
	Ship/Barge	Atmospheric	P
		Pressurized	P
Loading/Unloading arm	Road	Atmospheric	P
		Pressurized	P
	Rail	Atmospheric	P
		Pressurized	P
	Ship/Barge	Atmospheric	P
		Pressurized	P

More specifically, LOC events are defined as the types of releases of materials and/or energy from process equipment and pipework, affecting each node. As shown in Table 9, based on the Methodology for identifying major accident hazards (MIMAH) procedure (Delvosalle et al., 2004a), a set of three LOC events (i.e., catastrophic rupture, breach, and puncture) is identified. Depending on the equipment class, these LOC events can have different features. Therefore, to account for specific factors such as release geometry, duration, magnitude, and conditions, LOC events are characterized by a set of one or more release modes (RM), which define the release conditions to be considered for each LOC and to be later modelled in Step 5 (e.g., "release of liquid at inlet conditions from a hole of 10 mm" is a possible RM for LOC3).

Guidance on the definition of the relevant RM is provided by the reference release classes (RCs) reported in Table 9. RCs specify some features of the release mode, but shall be completed with information on the pre-release conditions (e.g., pressure, temperature, phase, and composition) to define a proper RM. More specifically, more than a single RM are usually defined when a RC may result in the release of significantly different streams from the same node. For example, in a typical liquid-vapor separator, three release modes of class RC5 need to be analyzed:a RM for the outlet liquid, a RM for the outlet vapor, and a RM for the inlet bi-phase.

Table 9
Loss of containment events, release classes, and their relationship with equipment classes (see from Table 4 to Table 8 for the definition of equipment classes).

LOC	RELEASE CLASS	EQUIPMENT CLASS			
		G_T	G_P	T	P
LOC1: Catastrophic rupture	RC1: Instantaneous release of the entire inventory	✓		✓	
	RC2: Release of the inventory in 10 min	✓		✓	
	RC3: Release of the nominal flow rates of all the inlet streams for 3 min		✓		✓
LOC2: Breach	RC4: Release from a hole of 50 mm	✓	✓	✓	✓
LOC3: Puncture	RC5: Release from a hole of 10 mm	✓	✓	✓	✓

While LOCs are the same for each node, the RCs to be considered depend on the equipment classes defined in Step 3 of the current methodology (see Section 3.3) as specified in Table 9.

3.5. Step 5: Calculation of damage distances

The fifth step of the methodology focuses on analyzing the consequences of LOC events, determining the damage distances associated with the end-point scenarios, which define the extent of the impact. This process begins with the identification of the end-point scenarios representing the possible hazardous outcomes of a RM, followed by the assessment of their consequences with respect to the targets considered.

3.5.1. Identification of end-point scenarios

End-point (accident) scenarios are determined for each reference RM using qualitative event trees derived from conventional approaches proposed in the technical literature (Delvosalle et al., 2004b; Mannan, 2012; TNO, 2005). The appropriate event tree shall be selected applying the conventional criteria used in risk analysis (see e.g., Mannan, 2012), considering the RM (i.e., the characteristics of the applicable RC and the expected operating conditions at the time of the release, categorized as in Table 10).

The results of the event trees are summarized in Table 11, where a list of baseline end-point scenarios requiring modelling are linked to both the selected release classes (see Table 9) and the corresponding physical states (defined in Table 10). Clearly enough, the list of end-point scenarios included in Table 11 should be considered as a baseline set to assure consistency to the analysis. However, on the one hand, further end-point scenarios may be added for specific substances and/or release classes. On the other hand, a baseline end-point scenario may be dropped in case it is not credible due to the specific properties of the substance and/or of the release class.

3.5.2. Calculation of damage distances for each end-point scenario

The calculation of the damage distances for each end-point scenario relies on the definition of damage threshold values of physical effects on humans, assets, and the environment (or other specific targets considered in the analysis). The damage distance is defined as the maximum radius from the point of the release at which the severity of the physical effect associated with the end-point scenario reaches the threshold value specified in Table 12 for the different targets (i.e., human, asset, environment) (Tugnoli et al., 2007).

The air compartment is not considered for environmental contamination in the present context, as substances tend to rapidly dilute

Table 10
Categorization of operating conditions at the time of release.

PHYSICAL STATE	DEFINITION
Liquid_1	Fluids with an operating temperature below the Normal Boiling Point (NBP), where NBP > T_{amb}
Liquid_2	Fluids with an operating temperature above the NBP, where NBP > T_{amb}, resulting in pressures higher than atmospheric
Pressurized gas	Fluids in the gaseous state maintained at a pressure above atmospheric pressure
Cryogenic liquid	Fluids liquefied at a temperature below their NBP, where NBP < T_{amb}
Liquefied gas with pressure	Fluids (typically at atmospheric temperature) liquefied at a pressure above their vapor pressure, where NBP < T_{amb}

Table 11
Baseline list of end-point scenarios (j) to be modelled according to the physical state and release class considered (VCE: Vapour Cloud Explosion; BLEVE: Boiling Liquid Expanding Vapor Explosion).

PHYSICAL STATE	RELEASE CLASS	Evaporating Pool	Boiling Pool	END-POINT SCENARIO						
				Fireball $j=1$	Jet-Fire $j=2$	Pool-Fire $j=3$	Flash-Fire $j=4$	VCE $j=5$	Toxic Cloud $j=6$	Burst/BLEVE $j=7$
Liquid_1	1	✓				✓	✓	✓	✓	Only for $P > P_{atm}$
	2,3,4,5	✓				✓	✓	✓	✓	
Liquid_2	1		✓	✓		✓	✓	✓	✓	✓
	2,3,4,5		✓		✓	✓	✓	✓	✓	
Pressurized gas	1			✓			✓	✓	✓	✓
	2,3,4,5				✓		✓	✓	✓	
Cryogenic liquid[a]	1		✓	✓		✓	✓	✓	✓	✓
	2,3,4,5		✓		✓	✓	✓	✓	✓	
Cryogenic liquid[b]	1,2,3,4,5		✓			✓	✓	✓	✓	**
Liquefied gas with pressure	1		✓*	✓		✓*	✓	✓	✓	✓
	2,3,4,5		✓*		✓	✓*	✓	✓	✓	

[a] Cryogenic liquid stored at a pressure higher than atmospheric pressure.
[b] Cryogenic liquid stored at a pressure near the atmospheric pressure.
[*] It has to be considered only for the rain-out formed after the fluid flash.
[**] Only in case of release above water of methane and possibly hydrogen (rapid phase transition).

Table 12
Damage threshold values related to the targets: human, asset, and the environment (Tugnoli et al., 2007).

END-POINT SCENARIO	EFFECT TYPE	THRESHOLD VALUE		
		HUMAN	ASSET	ENVIRONMENT
Flash-Fire	Heat radiation	½ LFL[a]	/	/
Fireball	Heat radiation	7 kW/m^2	15 kW/m^2	/
Jet-fire	Heat radiation	7 kW/m^2	15 kW/m^2	/
Pool-fire	Heat radiation	7 kW/m^2	15 kW/m^2	/
Vapor Cloud Explosion	Blast wave overpressure	14 kPa	16 kPa	/
Physical explosion	Blast wave overpressure	14 kPa	16 kPa	/
Toxic Cloud	Acute toxicity	IDLH[b]	/	/
Water/soil pollution	Acute toxicity	/	/	PNEC[c]

[a] LFL, Lower Flammability Limit [ppm].
[b] IDLH, Immediately Dangerous to Life and Health concentration [ppm].
[c] PNEC, Predicted No Effect Concentration [mg/l] (Crivellari et al., 2021b).

(Mannan, 2012). Additionally, the current methodology does not account for potential seafloor contamination, as the focus is on the onshore infrastructure. Specific details regarding seafloor impacts can be found elsewhere (Crivellari et al., 2021b; Di Talia et al., 2024; Tamburini et al., 2024a, 2023). Also in this case, Table 12 provides baseline threshold values needed to assure consistency to the analysis. Further threshold values may be added in case other environmental compartment or specific environmental targets are considered.

For the sake of simplicity, from now on, the methodology is described only referring to the human target. However, the same steps apply to all the other targets considered.

To model the physical effects of the end-point scenarios identified in Section 3.5.1 (see Table 11), integral consequence analysis models, along with software tools such as PHAST (DNV, 2025), EFFECTS (Gexcon, 2025), OLGA (Schlumberger, 2025), and ALOHA (US EPA, 2024), can be used. The potential occurrence of domino effects (Cozzani and Reniers, 2021) is not included in the calculation of the damage distances.

In order to assure consistency in the results, the modelling assumptions introduced need to be applied consistently thorough the analysis. In particular, the same model shall be applied to assess the damage distance of the same category of end-point scenarios. Moreover, the same weather conditions need to be applied in the calculation. In the case study carried out in the following, the integral models implemented in PHAST version 9.11 (DNV, 2025) were used. Weather conditions were restricted to a single case, deemed to be a worst-case scenario for dispersion phenomena: Pasquil stability class F, wind speed 1.5 m/s at 10 m elevation, air and ground temperature 10 °C, flat terrain, 70 % relative humidity. In case of release modes of class RC3, given the short duration of the release (i.e., 3 min) a puff model is considered for consequence analysis of end-point scenarios involving cloud dispersion phenomena. Clearly enough, the user can select different models and/or assumptions, provided they are applied consistently throughout the analysis.

Since integral models for consequence analysis tend to be unreliable in the "near-field" of the release location, the following criterion must be applied to determine the effective damage distance:

$$d^{eff}_{s,m,k,i,g,j} = \max\left(d^{calc}_{s,m,k,i,g,j}, 5\,m\right) \quad (2)$$

By the procedure described above, damage distances are obtained for each of the j^{th} end-point scenario related to the g^{th} release mode of the i^{th} LOC of the k^{th} node included in the m^{th} unit of the s^{th} system is the calculated damage distance, denoted as $d^{calc}_{s,m,k,i,g,j}$. The procedure shall be repeated for all the release modes, all the nodes, all the units, and all the systems considered.

A damage vector is then obtained considering the maximum damage distances among all the end-point scenarios for all the RMs of each LOC:

$$h_{s,m,k,i} = \max_{g,j}\left(d^{eff}_{s,m,k,i,g,j}\right) \quad (3)$$

3.6. Step 6: Assignment of credit factors

The sixth step of the methodology involves assigning a credit factor to each LOC event considered (c_{f_i}). The credit factors reflect the equipment inherent proneness to cause releases, representing the operational hazard of each equipment item. Notably, c_{f_i} is independent of the specific release modes actually considered in each LOC.

The determination of the credit factors relies on the analysis of baseline failure frequency databases and of specific literature data. It is linked to the taxonomy established in Step 2 of the current methodology (refer to Section 3.3). A database of suggested credit factors was developed in the present study and is reported in Appendix A (from Table A1 to Table A5).

Calculating credit factors for transport and transfer units as well as for batch processes needs additional specifications. In particular, in the case of pipelines, credit factors are obtained multiplying the length of

the pipeline by a baseline credit factor per unit length ($c_{f_{km}}$), which varies depending on the pipeline diameter. The recommended baseline credit factors values per unit length are provided in a dedicated database in Appendix A (see Table A4). Clearly enough, when a pipeline consists of multiple sections with different diameters, the length of each section must be multiplied by the corresponding credit factor value.

In the case of rail, road, and ship/barge tankers, the length of a single trip, L_v (km/trip), and the total number of trips per year, n (trip/y), are used to obtain the credit factor c_{f_y} (y^{-1}), as follows:

$$c_{f_y} = c_{f_{km}} \bullet L_v \bullet n \tag{4}$$

where $c_{f_{km}}$ ($y^{-1}km^{-1}$) is the failure frequency per unit length reported in Table A4 of Appendix A.

The total number of trips per year, n, is calculated as the ratio of the production capacity, p_u (kg/y), of the transport unit, to the transport capacity, C (kg), of the tanker node.

In the case of transfer units, credit factors are obtained multiplying the number of transfers per year (i.e., operations) by the unit factors given in Table A5 of Appendix A.

In the case of seasonal or batch processes, the credit factor must be modified as follows to take into account the actual yearly period of operation of batch nodes:

$$c_{f_{y_{eff}}} = c_{f_y} \bullet \frac{\tau_B}{\tau_y} \tag{5}$$

where c_{f_y} is the baseline credit factor available for continuous operation (see Appendix A, from Table A2 to Table A5), τ_B (h/y) is the time of use of the batch node, and τ_y is the number of hours in a year (8766 h/y).

3.7. Step 7: Calculation of indicators

In this step of the methodology, the inherent safety KPIs introduced in Section 3.1.5 are calculated, first at a node level, then at the level of the unit and of the system. The KPIs are calculated using the damage vector obtained in Step 5 of the methodology (see Section 3.5) and of the credit factors assigned to each LOC in Step 6 (see Section 3.6). It is important to ensure that all nodes and all units have been analyzed before proceeding with the KPI calculation. The procedure to calculate the KPIs is described in the following.

3.7.1. Calculation of KPIs at node level

The calculation of the potential and hazard indicators for each node shall be performed as detailed in Table 13.

In the case of rail, road, and maritime tanker transport, the calculation for each node (as defined in Step 3) incorporates specific features that account for the number of trips and tankers involved.

First, the mean trip time, τ_v (h/trip), shall be calculated as the ratio between the length of a single trip, L_v (km/trip), and the mean velocity, v_m (km/h), of the node. Then, a corrective factor, σ, is introduced to account for both the fraction of the year during which a tanker is in transit and the number of tankers required:

$$\sigma = \frac{\tau_v}{\tau_y} \bullet n \tag{6}$$

where τ_y is the number of hours in a year (8766 h/y) and n is the number of trips per year (see Section 3.6).

Finally, the KPI is computed as follows, encompassing the overall impact of transportation dynamics on system performance:

$$NPI_{s,m,k} = \sigma \bullet \left[\pi \max_i \left(h_{s,m,k,i}\right)^2\right] \tag{7}$$

3.7.2. Calculation of indicators at unit and system level

The calculation of the potential and hazard indicators for each unit consists of a summation of the KPIs obtained for the nodes composing the unit:

$$UPIH_{s,m} = \sum_{k=1}^{K} NPIH_{s,m,k} \tag{8}$$

$$UHIH_{s,m} = \sum_{k=1}^{K} NHIH_{s,m,k} \tag{9}$$

where K is the total number of nodes in unit m of system s.

The KPIs of each system are calculated considering its production capacity, P. Their calculation consists of a summation of the KPIs obtained for the units composing the system, weighted by their utilization fractions, $f_{u,s,m}$:

$$SPIH_s = \sum_{m=1}^{M} UPIH_{s,m} \bullet f_{u,s,m} \tag{10}$$

$$SHIH_s = \sum_{m=1}^{M} UHIH_{s,m} \bullet f_{u,s,m} \tag{11}$$

where M is the total number of units in system s and $f_{u,s,m}$ is the utilization factor calculated in Section 3.1.4 (see Eq. 1).

3.7.3. Calculation of hazard-specific indicators

Hazard-specific indicators may be calculated to obtain a hazard footprint specifically addressing fire, explosion, or toxicity hazards in order to explore specific hazard profiles according to the goal of the analysis. Three hazard-specific indices may be calculated, as shown in Table 14:

1. NFHIH: Node Flammability inherent Hazard index for Human target, addressing the hazard related to fire scenarios.
2. NOHIH: Node Overpressure inherent Hazard index for Human target, addressing the hazard due to blast waves.
3. NTHIH: Node Toxicity inherent Hazard index for Human target, addressing the hazard due to acute toxicity.

The calculation of these indicators follows rules similar to the general inherent hazard index (Step 7), but the generic damage vector $h_{s,m,k,i}$ (obtained in Step 5 of the methodology) is substituted by hazard-specific vectors which accounts only for the damage distance for the physical effect of concern (i.e., heat radiation, overpressure, acute toxicity). The specific equations are shown in Table 14. It shall be noted that the damage distances required for the quantification of the hazard-specific indicators were already evaluated in Step 5 and therefore no further calculation is required for the consequences of the end-point scenarios.

Table 13
Calculation of the potential and hazard KPIs at node level (H: Human; A: Assets; E: Environment).

GROUP	KPI	EQUATION	TYPE OF INDICATOR
H	NPIH	$NPIH_{s,m,k} = \pi \max_i \left(h_{s,m,k,i}\right)^2$	POTENTIAL
	NHIH	$NHIH_{s,m,k} = \pi \sum_{i=1}^{3} \left(c_{f_i} \bullet h_{s,m,k,i}^2\right)$	HAZARD
A	NPIA	$NPIA_{s,m,k} = \pi \max_i \left(A_{s,m,k,i}\right)^2$	POTENTIAL
	NHIA	$NHIA_{s,m,k} = \pi \sum_{i=1}^{3} \left(c_{f_i} \bullet A_{s,m,k,i}^2\right)$	HAZARD
E	NPIE	$NPIE_{s,m,k} = \pi \max_i \left(B_{s,m,k,i}\right)^2$	POTENTIAL
	NHIE	$NHIE_{s,m,k} = \pi \sum_{i=1}^{3} \left(c_{f_i} \bullet B_{s,m,k,i}^2\right)$	HAZARD

3.8. Step 8: Analysis of the results

The KPIs obtained from the above-described methodology are

Table 14
Calculation of the hazard-specific KPIs at node and unit level (*j*: label of the end-point scenario in Table 11).

HAZARD TYPE	DAMAGE VECTOR	KPI (node)	KPI (unit)
Heat radiation $j = 1 \div 4$	$f_{s,m,k,i} = \max\left[d^{eff}_{s,m,k,i,g,j}\right]$	$NFHIH_{s,m,k} = \pi \sum_{i=1}^{3} \left(c_{fi} \bullet f^{2}_{s,m,k,i}\right)$	$UFHIH_{s,m} = \sum_{k=1}^{K} UFHI_{s,m,k}$
Blast wave overpressure $j = 5$	$o_{s,m,k,i} = \max\left[d^{eff}_{s,m,k,i,g,j}\right]$	$NOHIH_{s,m,k} = \pi \sum_{i=1}^{3} \left(c_{fi} \bullet o^{2}_{s,m,k,i}\right)$	$UOHIH_{s,m} = \sum_{k=1}^{K} UOHI_{s,m,k}$
Acute toxicity $j = 6$	$t_{s,m,k,i} = \max\left[d^{eff}_{s,m,k,i,g,j}\right]$	$NTHIH_{s,m,k} = \pi \sum_{i=1}^{3} \left(c_{fi} \bullet t^{2}_{s,m,k,i}\right)$	$UTHIH_{s,m} = \sum_{k=1}^{K} UTHI_{s,m,k}$

interpreted to assess the overall inherent safety of the system, to compare alternative systems, and to identify critical units or nodes. Examples are provided in Section 5, reporting the results of the analysis of the case study introduced in Section 4.

In this step, the analysis of results is not limited to the deterministic interpretation of KPIs, but is extended to account for uncertainty and sensitivity. A probabilistic framework based on Monte Carlo simulation is proposed, whereby damage distances predicted by consequence models are perturbed using a multiplicative Gaussian error (sigma equal to 25 % of the nominal value, corresponding to a model error of approximately ± 50 % at two standard deviations). This procedure generates distributions of KPIs rather than single-point estimates, allowing confidence intervals and exceedance probabilities to be quantified. In parallel, sensitivity analysis highlights which uncertain parameters drive the largest share of output variability. Together, these complementary analyses provide a more transparent and defensible assessment of inherent safety, identify model assumptions that critically influence conclusions, and support decision-makers in prioritizing system modifications or further data collection. Clearly enough, the user may select alternative and case-specific methods for uncertainty and sensitivity analysis. Nevertheless, it is recommended that such analyses are carried out as part of the analysis of the results.

4. Case study

A case study has been defined to demonstrate the implementation of the methodology and the results obtained. The case study concerns two alternative systems for renewable energy supply to empower a ceramic manufacturing plant: biogas production from anaerobic digestion and hydrogen (H_2) production via electrolysis. The ceramic plant has a total energy demand of 3.28 GJ/t, thus considering the lower calorific values of natural gas (36.6 MJ/Nm^3) and hydrogen (10.8 MJ/Nm^3) (Kahangamage et al., 2024), 754 Nm/h of natural gas or 2557 Nm/h of hydrogen are necessary to meet the required energy input. In order to limit the complexity of the case-study, the inherent safety analysis of the ceramic manufacturing plant is out of scope of the case-study. The system boundary has been set at the furnace where biogas or hydrogen are burned to supply the required process heat. It should be remarked that, since the configuration of the manufacturing plant remains identical in both supply options, its inherent safety performance does not affect the comparative assessment of the renewable energy supply chain.

4.1. System 1: biomethane-based value chain

The local production of biomethane (BioM) involves a preliminary anaerobic digestion system for biomass, followed by a desulfurization and upgrading system (Calise et al., 2021; Carvalho et al., 2023), as shown in the PFD in Fig. 3.

Initially, a filter removes solid and liquid impurities before the biogas enters a scrubbing column, where sodium hydroxide (NaOH) and water (H_2O) act as solvents to completely eliminate hydrogen sulfide (H_2S) (Castellanos-Sánchez et al., 2024). The column integrates an oxidation tank that oxidizes H_2S into elemental sulfur, enabling the recovery of NaOH and H_2O (Dumont, 2015). Since this equipment does not involve hazardous substances, it has been neglected for the inherent safety assessment. A condenser, using cooling fluid from a refrigeration cycle, then lowers the biogas temperature from approximately 40 °C to 5 °C, facilitating dehumidification (Calise et al., 2021). Further purification occurs via an activated carbon filter, ensuring the removal of residual acidic gases and liquid impurities. The conditioned biogas is subsequently compressed to 2 MPa and directed to a selective membrane (Gkotsis et al., 2023), where 669 Nm^3/h of carbon dioxide (CO_2) (with 0.66 % of methane (CH_4)) permeates for collection and storage, while CH_4 is retained at a significantly lower rate, yielding a purified (97 %) biomethane stream having a medium hourly production rate of 903 Nm^3. The retentate is then transported to the ceramic furnace through a buried pipeline, 2 km long and 3 in in diameter.

Detailed information about operating conditions (i.e., temperature and pressure), compositions, mass flow rates, and inventories are reported in Table S1 in the Supplementary Material.

As shown in Fig. 3, the biomethane value chain is divided into five units, each comprising various nodes as summarized in

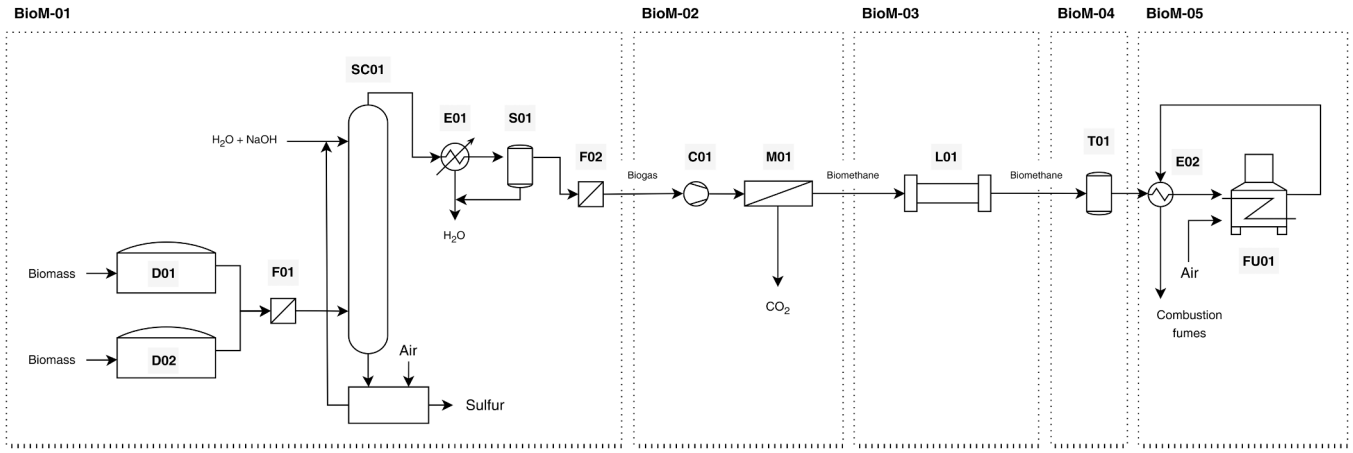

Fig. 3. PFD of the biomethane-based value chain with a focus on the identified units (BioM-01-BioM-05) (refer to Table S1 in the Supplementary Material for node tag definitions).

Table 15
Classification of units and nodes of the local biomethane-based value chain.

UNIT	DESCRIPTION	NODE	CLASS
BioM-01	Biogas production	D01 – D02	G_T
		F01	G_P
		SC01	G_P
		E01	P
		S01	G_P
		F02	G_P
BioM-02	Upgrading	C01	P
		M01	G_P
BioM-03	Biomethane transport	L01	P
BioM-04	Biomethane storage	T01	T
BioM-05	Final user	E02	P
		FU01	P

Table 15—except for the third and fourth units, which consists of a single node.

4.2. System 2: Hydrogen-based value chain

The local production of hydrogen relies on an electrolysis system in which water is separated into oxygen (O_2) and hydrogen (Arsad et al., 2023), as illustrated in the PFD in Fig. 4.

More in detail, a total of 12 electrolyzers operating in parallel is necessary to meet the required hourly H_2 flow rate of 2557 Nm^3. This setup ensures a consistent and efficient production of H_2 to satisfy the plant's energy demand. The electrolyzers are of the alkaline type, based on a potassium hydroxide (KOH) solution (Tüysüz, 2023), and each has a power capacity of approximately 1 MW.

As illustrated in the PFD (see Fig. 4), H_2O is first introduced into the system and undergoes pre-treatment in separation units before being fed into the electrolyzer stack (Cammann et al., 2024). Within the electrolyzer, H_2O is split into H_2 and O_2, with the hydrogen stream passing through multiple purification and drying stages—including separation, cooling, and moisture removal—to ensure high-purity gas output (Sakas et al., 2022). The produced H_2 is subsequently compressed and stored at 50 bar and 25 °C, with a residence time of 12 h, while the O_2 by-product is safely vented.

It is worth noting that, for the purpose of comparison between hydrogen and biomethane production, air was assumed as the combustion agent in the ceramic furnace.

Comprehensive data on operating conditions (i.e., temperature and pressure), compositions, mass flow rates, and inventories can be found in Table S2 in the Supplementary material. Pumps and filters, handling only H_2O and free from hazardous substances, have been excluded from the inherent safety assessment.

Within the H_2 production plant (see Fig. 4), three units have been identified, each comprising various nodes as summarized in Table 16—apart from the second unit, which contains just a single node.

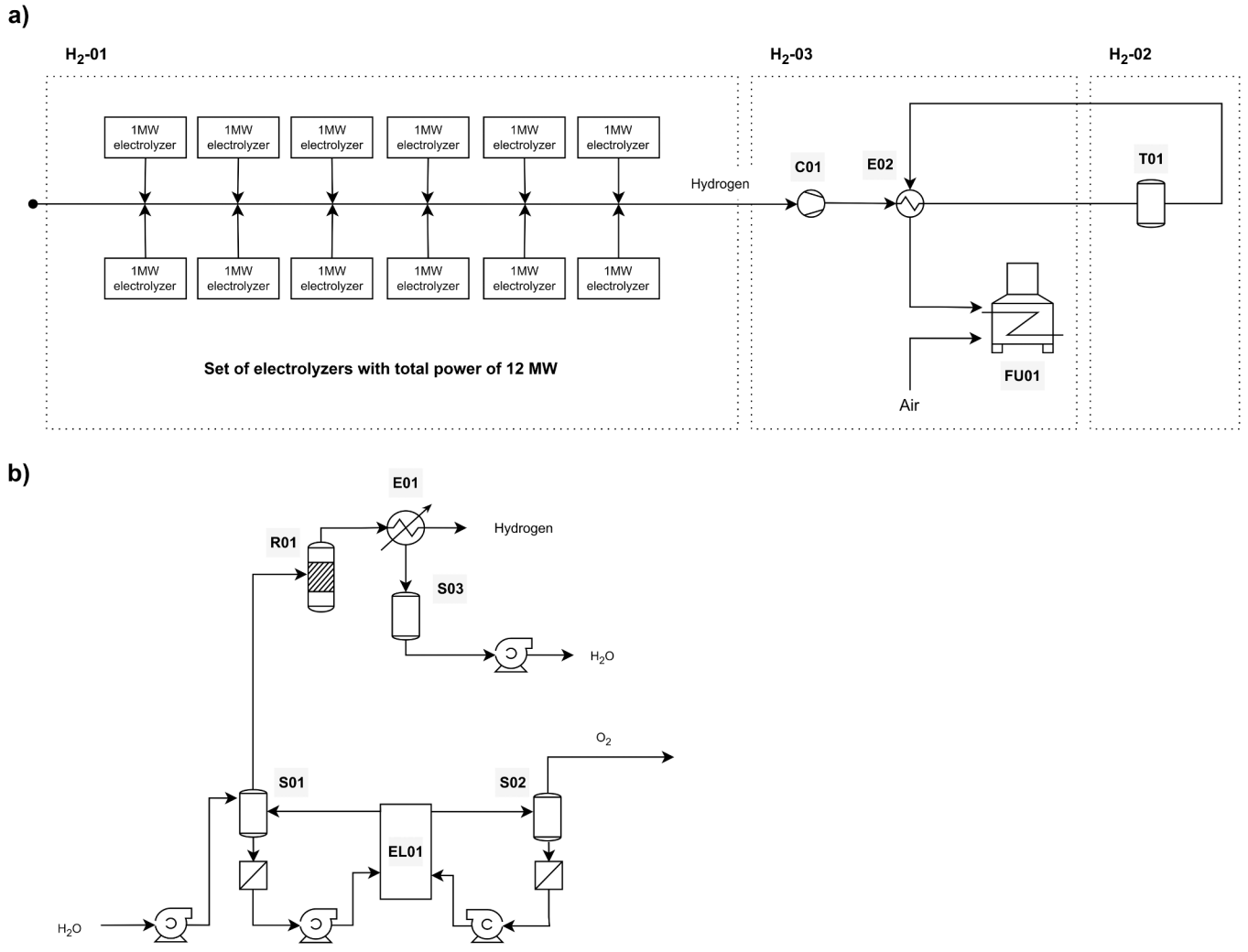

Fig. 4. a) PFD of the hydrogen-based value chain with a focus on the identified units (H_2-01-H_2-03); b) Detailed process flow diagram of a single electrolyzer system constituent of H_2-01 (refer to Table S2 in the Supplementary Material for node tag definitions).

Table 16
Classification of units and nodes of the local hydrogen-based value chain.

UNIT	DESCRIPTION	NODE	CLASS
H_2-01	Hydrogen and Oxygen production	S01–1 – S01–12	G_P
		S02–1 – S02–12	G_P
		S03–1 – S03–12	G_P
		E01–1 – E01–12	P
		EL01–1 – EL01–12	G_T
		R01–1 – R01–12	G_P
H_2-02	Hydrogen storage	T01	T
H_2-03	Final user	C01	P
		E02	P
		FU01	P

5. Results and discussion

5.1. Results of the case study

The results obtained by the application of the ExALIS methodology to the case study are presented and discussed in the following.

Table 17 reports the KPIs calculated for one of the nodes corresponding to a specific unit: the hydrogen storage node (T01), which coincides with unit H_2-02. The table summarizes the main parameters derived from the different steps of the methodology, including the LOC events, the RMs, the corresponding credit factors, the end-point scenarios, and the damage distances and vectors, together with the calculated values of NPIH/UPIH and NHIH/UHIH. These KPIs were assessed using the equations reported in Table 13, taking into account the assigned credit factors and the estimated damage distances for each scenario. Among the analyzed end-point scenarios, the Fire-Ball shows the largest damage distance for RM1, whereas the VCE results in the greatest damage distances for all the other release modes, followed by the Flash-Fire scenario.

Building on the results of the node-level analysis, a system-wide perspective is developed. The results from individual nodes are aggregated based on Eqs. 10 and 11 to evaluate the overall performance of the two value chains. Fig. 5 compares the SPIH (see Fig. 5a)) and the SHIH (see Fig. 5b)) indices for both value chains, also showing the decomposition of the system-level indices into contributions from individual units.

In both value chains, the dominant hazard affecting human health is associated with flammability, given the inherent hazardous characteristics of biomethane and hydrogen. As shown in Fig. 5a), the biomethane-based value chain exhibits a markedly higher value of the SPIH (around 430000 m^2) compared to hydrogen (around 320000 m^2), indicating a higher potential for human exposure across the system. As evident also from Fig. 6a), showing the detail of the UPIH indices calculated for the biomethane system, the difference is primarily due to unit BioM-04 (i.e., biomethane storage) in the biomethane pathway, which alone contributes nearly to 80 % of the SPIH for biomethane, suggesting that the storage is a major hotspot in terms of hazard potential. In the case of the hydrogen-based value chain, Fig. 5a) and Fig. 6b) show that H_2-02 (i.e., hydrogen storage) plays as well the most relevant role, but the overall contributions are significantly lower and more evenly distributed with respect to the biomethane-based value chain. Moreover, the results show the importance of adopting a system approach in the inherent safety assessment: if only the end-use units (BioM-05 and H_2-03) is considered, a lower score is obtained for the biomethane option, while the system perspective evidences a shift of the hazard toward other units of the value chain.

Fig. 5b) presents the SHIH values, which, unlike SPIH, incorporate both the damage distances and the failure frequencies, providing a more detailed estimation of credible hazards. The SHIH value of the H_2 system results of approximately 25 m^2/y, far exceeding that of biomethane, which is of about 3 m^2/y. In this case, unit H_2-01 (i.e., Hydrogen and Oxygen production) is the dominant contributor in the H_2 pathway. This is confirmed also by Fig. 6d), that reports the details of the UHIH values calculated for the H_2 system. These results suggest that the electrolyzer stacks are associated with the highest hazard in the system. When considering the SHIH distribution in the biomethane system, both Fig. 5b) and Fig. 6c) show a safer and more uniformly distributed hazard profile compared to hydrogen system. In both chains, the end-use units (BioM-05 and H_2-03) show a limited and comparable impact on the final KPI values.

Examining the individual units in more detail, the UPIH and UHIH indices can be decomposed into the contributions of each node. As an example, Fig. 6e) and Fig. 6f) show the node contributions, expressed as the NPIH indices, for two representative units: BioM-01 and H_2-01. As evident from Fig. 6e), the high value of the SPIH index obtained for the biomethane-based value chain largely derives from the NPIH of the digesters (node D01–D02). Conversely, in the case of unit H_2-01, Fig. 6f) shows that the electrolyzers (node EL01–1–EL01–12) provide the highest contribution to the overall SPIH, with other nodes (S02–1–S02–12, R01–1–R01–12, S01–1–S01–12, and S03–1–S03–12) contributing more evenly.

Additional insights can be obtained by examining the footprint of hazard-specific KPIs at the node level (see definitions in Table 13). In this context, Fig. 7 illustrates the contributions of the different scenarios related to toxicity (NTHIH) and flammability (NFHIH) indices in unit BioM-01. Results are reported only for unit BioM-01, as this is the only unit in the case study exhibiting contributions from both toxicity- and flammability-driven scenarios.

As shown in Fig. 7, the relative contributions of the toxicity- and flammability-related indices vary significantly across nodes. Node S01 exhibits the highest overall NHIH value, driven mainly by its significant

Table 17
Hydrogen storage (Node: T01 = Unit: H_2-02): LOC, RM, credit factor, end-point scenario, damage distance, damage vector, NPIH/UPIH, and NHIH/UHIH. See Section 3.4 and Table 9 for the definition of LOC and RM (VCE: Vapor Cloud Explosion; BLEVE: Boiling Liquid Expanding Vapor Explosion).

LOC	RM	Credit factor [y^{-1}]	End-point scenario [m]	Damage distance [m]	Damage vector [m]	NPIH/ UPIH [m^2]	NHIH/ UHIH [m^2/y]
LOC1*	RM1	9.5×10^{-7}	Flash-Fire	76	241	182467	0.25
			VCE	205			
			Fire-Ball	241			
			BLEVE	135			
	RM2	9.5×10^{-7}	Flash-Fire	70			
			VCE	73			
			Jet-Fire	40			
LOC2**	RM4.1	3.7×10^{-6}	Flash-Fire	71	73		
			VCE	73			
			Jet-Fire	41			
LOC3**	RM5.1	6.9×10^{-6}	Flash-Fire	20	26		
			VCE	26			
			Jet-Fire	8			

*RM3 not applicable for a storage node (no nominal feed flowrate) **RM referred only to the release at the higher operative pressurize conditions (safe side for lower operative pressures).

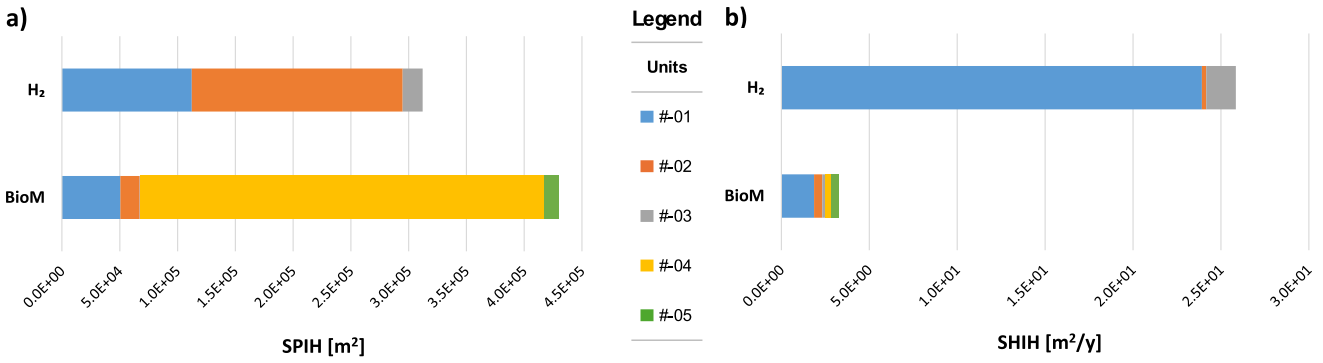

Fig. 5. Comparison between a) the SPIH and b) the SHIH indices for the two systems, embodying alternative value chains, considered in the case study: biomethane (BioM) and hydrogen (H_2). The stacked bar charts highlight the contributions of the different units to the overall SPIH and SHIH.

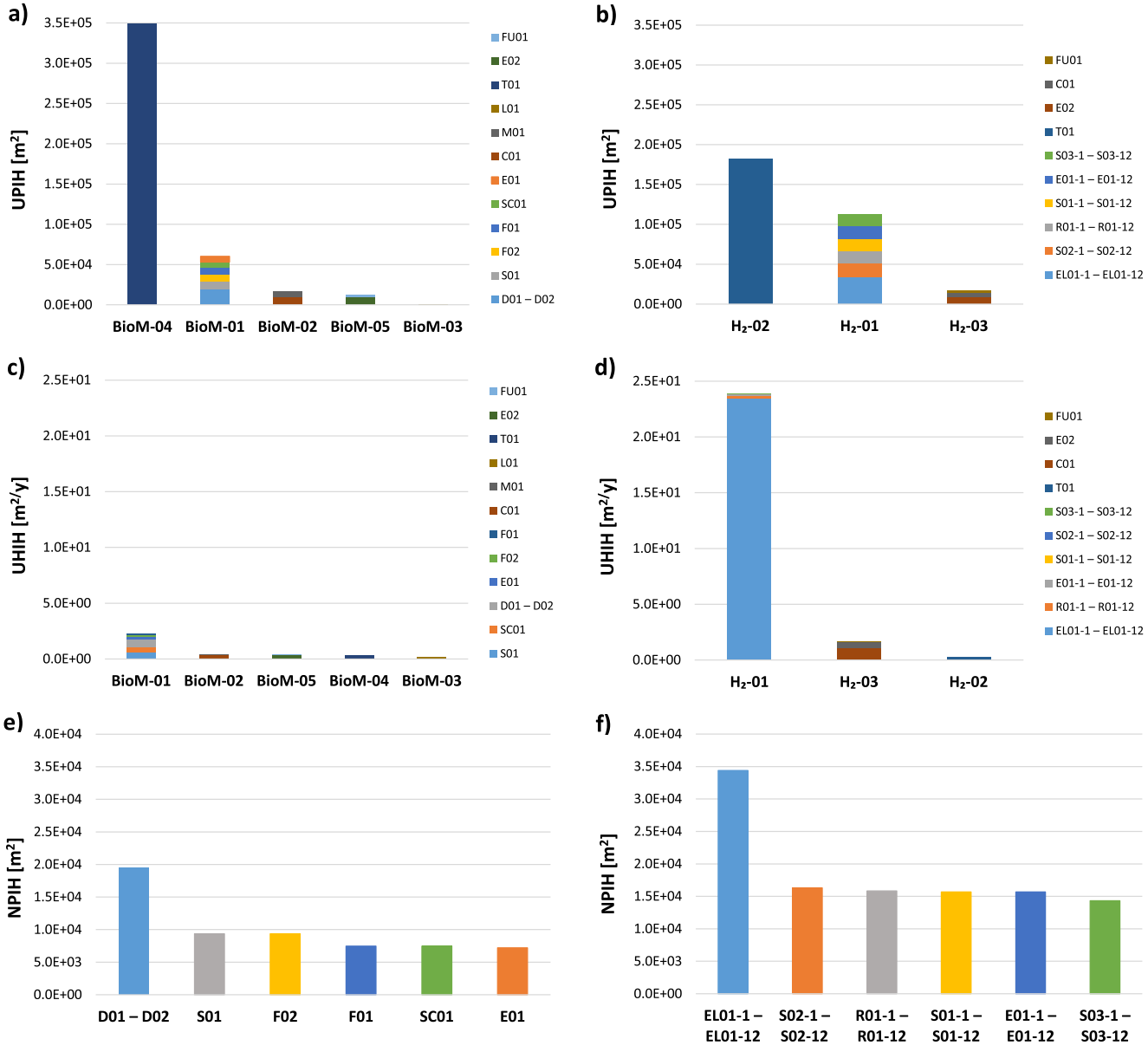

Fig. 6. Values of the: a) UPIH indices calculated for the units of the BioM system; b) UPIH indices calculated for the units of the H_2 system; c) UHIH indices calculated for the units of the BioM system; d) UHIH indices calculated for the units of the H_2 system; e) NPIH indices calculated for the nodes of the BioM-01 Unit; f) NPIH indices calculated for the nodes of the H_2-01 Unit (see Table 15 and Table 16 for nodes definition).

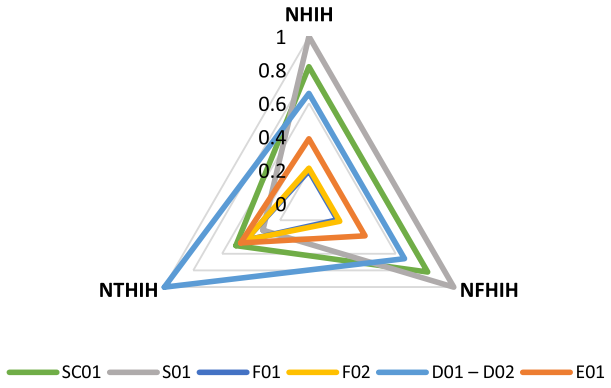

Fig. 7. Normalized node inherent hazard indices for human targets in unit BioM-01. The specific contributions of scenarios caused by toxicity (NTHIH) and flammability (NFHIH) hazard are also shown.

flammability-related contribution, whereas node D01–D02 displays a more pronounced toxicity-driven profile. SC01 shows a balanced contribution from both hazard types, while F02 and E01 present the lowest normalized indices, indicating minor influence on the overall unit hazard profile. This differentiation highlights the non-uniform distribution of the hazard potential within the units, emphasizing the importance of a node-specific analysis to prioritize safety improvements.

Finally, a Monte Carlo–based sensitivity analysis was carried out to evaluate the influence of the uncertainty associated with the consequence analysis of end-point scenarios on the overall SHIH. The epistemic uncertainty in each consequence analysis model applied for a specific end-point scenario (i.e., Fire-Ball, VCE, BLEVE, Jet-Fire, Flash-Fire, Toxic Cloud) was assessed, to understand the effect on the damage distances, that are the crucial aspect of the model. A normally distributed multiplicative factor (mean = 1, standard deviation = 0.25) was assigned to each end-point scenario type. The analysis was performed assuming a systematic-type error approach, aimed at quantifying the effect of model bias on the final hazard metric.

The results, visualized as tornado-chart-style plots in Fig. 8, revealed that for both biomethane (Fig. 8a)) and hydrogen (Fig. 8b)) value chains, the Fire-Ball scenario is the dominant contributor to the overall SHIH uncertainty. In the case of hydrogen, the VCE scenario also plays a significant role, contributing to 34.9 % of the variance, whereas BLEVE, Jet-Fire, and Flash-Fire have minor influences. In the biomethane chain, the contribution of VCE is smaller, and other scenarios, including BLEVE, Jet-Fire, Flash-Fire, and Toxic Cloud, provide a negligible contribution. These findings highlight that efforts to reduce uncertainty in Fire-Ball modeling are critical for both energy carriers, while improving VCE modeling is particularly relevant for correct assessment of hydrogen hazards. Overall, the sensitivity analysis provides a clear guidance for prioritizing the refinement of consequence models to enhance confidence in HIH estimates.

5.2. Discussion

Overall, the ExALIS tool provided a thorough assessment of the inherent safety of systems embodying alternative value chains, allowing both the specific assessment of the safety criticalities of each system and a comparison among the expected safety performance of the alternative systems considered. The results revealed that both the biomethane and hydrogen value chains entail a notable potential for human exposure, primarily due to the contribution of storage units. However, this potential was more pronounced in the biomethane-based system. Conversely, the hydrogen system exhibited a significantly higher inherent hazard to humans, mainly because of the operating hazards associated with the electrolyzer stack, which dominate the risk profile of the system. Overall, the higher inherent hazard outweighs the reduction in human exposure, making the biomethane route the safer option from an inherent safety perspective. Consequently, when adopting an inherent safety perspective, the biomethane-based option is identified as the preferred and more advisable alternative for renewable energy supply to implement.

The application of ExALIS to the case study demonstrated the robustness and versatility of the proposed approach, as well as its flexibility and compatibility with existing design workflows. ExALIS showed particular added value in early-stage process development, especially when dealing with emerging technologies. In such contexts, conventional safety assessment methodologies (e.g., Hazard and Operability Analysis, Process Hazard Analysis, Layer of Protection Analysis, Quantitative Risk Assessment (ISO, 2018, 2016)) typically require data that are not yet available in early design phases. In this regard, the ex-ante inherent safety KPIs generated by ExALIS can be regarded as leading indicators that support informed decision-making during the conceptual and preliminary stages of design.

Further validation across a wider range of industrial sectors would enhance the generalizability of the methodology and promote its integration into both industrial and policy decision-making processes.

Future work may also explore new comparative assessment scenarios, such as evaluating alternative configurations—local versus centralized—within the same technological value chain. This would help clarify how distribution and infrastructure choices influence trade-offs

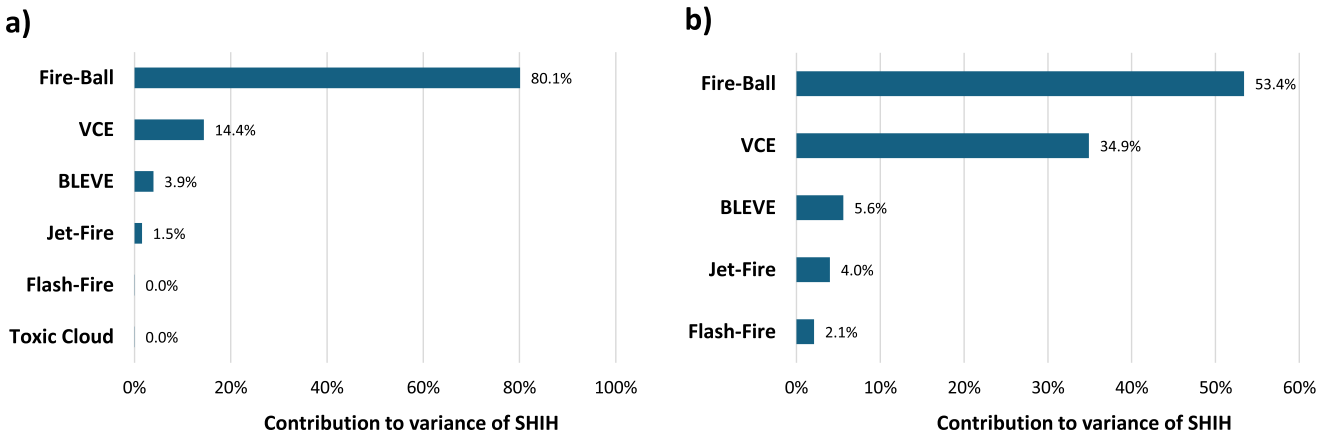

Fig. 8. Results of the Monte Carlo–based sensitivity analysis of SHIH on damage distances calculated for each end-point scenario (Fire-Ball, VCE, Flash-Fire, BLEVE, Toxic Cloud, Jet-Fire): a) BioM and b) H_2 system (VCE: Vapor Cloud Explosion; BLEVE: Boiling Liquid Expanding Vapor Explosion).

between safety and sustainability. Additionally, there is potential to broaden the scope of hazard indicators within the ExALIS framework by incorporating socio-economic risk factors, domino effects, and aspects related to circular economy models.

Finally, integrating ExALIS with dynamic simulation tools and digital design environments (e.g., digital twins and process simulators) could further enhance its responsiveness to real-time data and operational variability, ultimately strengthening its role as a decision-support tool for safe and sustainable process development.

6. Conclusions

The ExALIS (Ex-ante Assessment of Life cycle Inherent Safety) tool developed in the present study is an innovative, consequence-based methodological approach designed to quantitatively assess inherent safety across entire industrial value chains from the earliest stages of process design. ExALIS adopts a quantitative, holistic, life cycle-oriented perspective that captures interdependencies among equipment, unit operations, and systems embodying supply chains, overcoming the limitations of conventional methods that focus narrowly on unit-level design and overlook complex, multi-tiered risks. This reduces the chance to neglect burden shift phenomena, where lowering the hazard of a particular unit of the value chain is outbalanced by introducing higher hazards in other units. Moreover, the perspective is expanded beyond the sole units required for the chemical process route, considering the whole of the units required for value chain implementations, also including storage, transport, auxiliary units.

ExALIS allows for proactive hazard identification and mitigation, significantly reducing the likelihood of costly retrofits and late-stage safety interventions. Its modular structure also permits seamless integration with environmental life cycle assessment, facilitating comprehensive trade-off analyses between safety, sustainability, and operational efficiency.

The application of ExALIS to a comparative case study in the ceramic sector, evaluating biomethane and hydrogen-based decarbonization pathways, demonstrates the robustness and versatility of the approach. It effectively informs strategic decision-making by showing systemic safety risks and their potential consequences across the value chain. The results reveal that both the biomethane and hydrogen value chains involve a notable potential for human exposure, primarily due to the contribution of storage units.

Overall, ExALIS proved a scalable and practical tool supporting the design of inherently safer and more sustainable industrial systems. Its flexibility and compatibility with existing design workflows make it particularly suited for early-stage process development in emerging technologies and complex industrial contexts.

CRediT authorship contribution statement

Federica Tamburini: Writing – original draft, Methodology, Investigation, Data curation, Conceptualization. **Lorenzo Pasquali:** Investigation, Formal analysis, Data curation. **Alessandro Dal Pozzo:** Validation, Methodology, Investigation, Conceptualization. **Alessandro Tugnoli:** Writing – review & editing, Validation, Methodology, Investigation, Data curation, Conceptualization. **Valerio Cozzani:** Writing – review & editing, Validation, Supervision, Methodology, Conceptualization.

Declaration of Competing Interest

The authors declare that they have no known competing financial interests or personal relationships that could have appeared to influence the work reported in this paper.

Acknowledgments

This work was undertaken as part of Project “Network 4 Energy Sustainable Transition”, PE00000021, CUPJ33C22002890007 funded by the Italian Ministry of University and Research under the National Recovery and Resilience Plan, Misson 4, Component 2, Investment 1.3, NextGenerationEU.

Appendix. Database of credit factors

A credit factor (c_f) quantifies the credibility of a loss of containment (LOC) event considered at a given node, reflecting the inherent operation hazard of the equipment. Derived from the analysis of baseline failure frequency databases and literature data, c_f provides a measure of the equipment’s proneness to release.

A comprehensive list of case-specific credit factors used in this methodology is presented in Table A2, Table A3, Table A4, and Table A5, aligned with the taxonomy established in Step 2 of the methodology (see Section 3.1.2). Table A1 provides a legend explaining the letters (in brackets) applied in Table A2, Table A3, Table A4, and Table A5, which describe the source data considered to obtain the values.

Table A1
Label legend explaining the failure frequency databases and literature data considered to obtain the values of the case-specific credit factors reported in Table A2, Table A3, Table A4, and Table A5. The letter is used to identify values derived from data sources different that standard.

LETTER	SOURCE DATA	REFERENCE
no indication (standard)	IOGP – Process Release Frequencies	(IOGP, 2019a)
	IOGP – Storage incident frequencies	(IOGP, 2022)
	IOGP – Riser & Pipeline Release Frequencies	(IOGP, 2010)
	IOGP – Blowout Frequencies	(IOGP, 2019b)
	TNO – PURPLE BOOK	(TNO, 2005)
	ARAMIS D1C APPENDIX 10 – Generic frequencies data for the critical events	(Delvosalle et al., 2004c)
	DNV – Failure frequencies guidance	(DNV, 2013)
	OREDA – Offshore reliability data handbook 4th edition	(OREDA, 2002)
(a)	HSE – Failure Rate and Event Data for use within Risk Assessments (06/11/17)	(HSE, 2017)
(b)	Flemish Government – Handbook Failure Frequencies	(Flemish Government, 2009)
(c)	PLOFAM(2) – Process Leak for Offshore Installations Frequency Assessment Model	(Fossan and Opstad, 2018)
(d)	Paper: “*Risk Uncertainty in the Transport of Hazardous Materials*” by F.F. Saccomanno, M. Yu & J.H. Shortreed	(Saccomanno et al., 1993)

(*continued on next page*)

Table A1 (*continued*)

LETTER	SOURCE DATA	REFERENCE
(e)	Paper: "*Comparative analysis of failure probability for ethylene cracking furnace tube using Monte Carlo and API RBI technology*" by W. Wang, K. Liang, C. Wang & Q. Wang	(Wang et al., 2014)
(f)	Values derived by proportioning with the storage tanks (process nodes), using a "characteristic time" (h/km) based on an average ship velocity of 13.9 knots.	-
(g)	Values obtained by comparison between compressors and turbines	-
(h)	Values based on expert judgment obtained by averaging data from other sub-categories of similar equipment	-

Table A2
LOC credit factors for process nodes (all-purpose). References for data sources are reported in Table A1.

PROCESS NODES (ALL PURPOSE)						
CATEGORY	**SUB-CATEGORY**		**LOC**			**UNITS**
			LOC1	**LOC2**	**LOC3**	
Process vessel	Columns	Atmospheric	5.0×10^{-5} (c)	1.7×10^{-4} (c)	2.6×10^{-4} (c)	y^{-1}
		Pressurized	3.0×10^{-7} (c)	9.3×10^{-5}	1.7×10^{-4}	
	Separators	Atmospheric	5.0×10^{-5} (c)	1.7×10^{-4} (c)	2.6×10^{-4} (c)	
		Pressurized	3.0×10^{-7} (c)	9.3×10^{-5}	1.7×10^{-4}	
	Filters	Atmospheric	1.6×10^{-6} (c)	1.5×10^{-4}	4.4×10^{-4}	
		Pressurized	1.6×10^{-6} (c)	1.5×10^{-4}	4.4×10^{-4}	
	Reactors	Stirred tank	1.0×10^{-5} (a)	9.3×10^{-5}	1.7×10^{-4}	
		Tubular	1.3×10^{-5} (b)	2.1×10^{-4}	4.3×10^{-4}	
	Others/Unspecified	Atmospheric	5.0×10^{-5} (c)	1.7×10^{-4} (c)	2.6×10^{-4} (c)	
		Pressurized	3.0×10^{-7} (c)	9.3×10^{-5}	1.7×10^{-4}	
Storage tank	Atmospheric		5.0×10^{-6}	2.2×10^{-4} (b)	3.0×10^{-4}	
	Pressurized		9.5×10^{-7}	3.7×10^{-6}	6.9×10^{-6}	
	Cryogenic		5.0×10^{-6}	2.7×10^{-4}	3.0×10^{-4}	
	Tank containers (ISO)		4.0×10^{-6} (a)	3.0×10^{-5} (a)	6.0×10^{-5} (a)	
Heat exchanger	Shell&Tube		1.3×10^{-5} (b)	2.1×10^{-4}	4.3×10^{-4}	
	Plates&Frames		1.1×10^{-5} (b)	6.8×10^{-4}	2.0×10^{-3}	
	Air-coolers		1.5×10^{-5} (c)	1.1×10^{-4}	3.1×10^{-4}	
	Furnaces/Boilers		6.6×10^{-7} (d)	3.6×10^{-6} (d)	8.9×10^{-7} (d)	
	Direct Fire Heaters		6.6×10^{-7} (d)	3.6×10^{-6} (d)	8.9×10^{-7} (d)	
	Others/Unspecified		1.3×10^{-5} (h)	3.3×10^{-4} (h)	9.1×10^{-4} (h)	
Machinery	Pumps (centrifugal)		3.0×10^{-5} (a)	1.8×10^{-5}	1.6×10^{-4}	
	Pumps (alternative)		3.0×10^{-5} (a)	4.5×10^{-4}	8.6×10^{-4}	
	Pumps (others/unspecified)		3.0×10^{-5} (h)	2.3×10^{-4} (h)	5.1×10^{-4} (h)	
	Compressors (centrifugal)		2.9×10^{-6} (a)	2.5×10^{-4}	9.2×10^{-4}	
	Compressors (alternative)		1.4×10^{-5} (a)	5.6×10^{-4}	2.0×10^{-3}	
	Compressors (others/unspecified)		8.5×10^{-6} (h)	4.1×10^{-4} (h)	1.4×10^{-3} (h)	
	Turbines		2.9×10^{-6} (g)	3.4×10^{-4}	1.1×10^{-3}	
Piping	Process piping	$D \leq 6''$	7.5×10^{-7} (a)	2.2×10^{-6}	5.2×10^{-6}	$m^{-1}\ y^{-1}$
		$6'' < D \leq 18''$	1.7×10^{-7} (a)	2.6×10^{-6}	4.5×10^{-6}	
		$D > 18''$	7.0×10^{-8} (a)	3.3×10^{-6}	4.9×10^{-6}	
	Permanently installed hoses	$D \leq 6''$	5.6×10^{-5} (c)	1.1×10^{-4}	1.8×10^{-4}	
		$6'' < D \leq 18''$	5.6×10^{-5} (c)	9.2×10^{-6}	1.0×10^{-5}	
		$D > 18''$	5.6×10^{-5} (c)	3.0×10^{-6}	2.9×10^{-6}	
	Temporary hoses	$D \leq 6''$	5.6×10^{-5} (c)	1.1×10^{-4}	1.8×10^{-4}	
		$6'' < D \leq 18''$	5.6×10^{-5} (c)	9.2×10^{-6}	1.0×10^{-5}	
		$D > 18''$	5.6×10^{-5} (c)	3.0×10^{-6}	2.9×10^{-6}	

Table A3
LOC credit factors for process nodes (specialized). References for data sources are reported in Table A1.

PROCESS NODES (SPECIALIZED)						
CATEGORY	**SUB-CATEGORY**		**LOC**			**UNITS**
			LOC1	**LOC2**	**LOC3**	
Oil&Gas	Wellhead (surface, subsea)		4.0×10^{-7} (c)	3.1×10^{-6} (c)	6.6×10^{-5} (c)	y^{-1}
	Pig trap (launcher, receiver)		3.4×10^{-5} (c)	4.1×10^{-4}	7.4×10^{-4}	
	Manifold, header	$D \leq 6"$	5.0×10^{-7} (a)	1.3×10^{-6}	4.8×10^{-6}	$m^{-1}y^{-1}$
		$6'' < D \leq 16''$	7.0×10^{-8} (a)	4.6×10^{-7}	1.9×10^{-6}	
		$D > 16''$	4.0×10^{-8} (a)	2.9×10^{-6}	6.2×10^{-6}	
	Riser (steel fixed)	$D \leq 16"$	2.0×10^{-4}	2.0×10^{-4}	3.0×10^{-4}	y^{-1}
		$D > 16''$	2.6×10^{-5}	2.6×10^{-5}	3.9×10^{-5}	
	Riser (flexible)	Overall	8.8×10^{-4}	1.3×10^{-4}	2.2×10^{-4}	
Hydrogen	Fuel cell		1.1×10^{-5}	6.8×10^{-4}	2.0×10^{-3}	
	Electrolyser		1.1×10^{-5}	6.8×10^{-4}	2.0×10^{-3}	
Venting system	Flare/Burner		6.6×10^{-7}	3.6×10^{-6}	8.9×10^{-7}	
	Venting&Blowdown system		3.0×10^{-7}	9.3×10^{-5}	1.7×10^{-4}	

Table A4
LOC credit factors for transport nodes. References for data sources are reported in Table A1.

TRANSPORT NODES						
CATEGORY	**SUB-CATEGORY**		**LOC**			**UNITS**
			LOC1	**LOC2**	**LOC3**	
Pipeline	Steel pipeline Offshore	D ≤ 6"	1.7×10^{-5}	5.7×10^{-5}	8.6×10^{-5}	$km^{-1}\ y^{-1}$
		6'' < D ≤ 10''	3.0×10^{-5}	9.9×10^{-5}	1.5×10^{-4}	
		10'' < D ≤ 16''	1.4×10^{-5}	4.8×10^{-5}	7.2×10^{-5}	
		D > 16''	1.6×10^{-6}	5.3×10^{-6}	8.0×10^{-6}	
	Oil pipeline Offshore	D ≤ 6"	8.9×10^{-5}	1.6×10^{-4}	7.5×10^{-5}	
		6'' < D ≤ 10''	6.7×10^{-5}	1.2×10^{-4}	5.6×10^{-5}	
		10'' < D ≤ 16''	5.3×10^{-5}	9.2×10^{-5}	4.3×10^{-5}	
		D > 16''	6.3×10^{-5}	1.1×10^{-4}	5.3×10^{-5}	
	Gas pipeline Onshore	D ≤ 6"	4.1×10^{-5}	6.2×10^{-5}	6.2×10^{-5}	
		6'' < D ≤ 10''	2.6×10^{-5}	3.9×10^{-5}	3.9×10^{-5}	
		10'' < D ≤ 16''	1.3×10^{-5}	2.0×10^{-5}	2.0×10^{-5}	
		D > 16''	9.1×10^{-6}	1.4×10^{-5}	1.4×10^{-5}	
Tankers	Road	Atmospheric	2.2×10^{-8} (e)	3.9×10^{-8} (e)	3.9×10^{-8} (e)	km^{-1}
		Pressurized	2.2×10^{-8} (e)	3.9×10^{-8} (e)	3.9×10^{-8} (e)	
	Rail	Atmospheric	6.7×10^{-9} (e)	1.2×10^{-8} (e)	1.2×10^{-8} (e)	
		Pressurized	6.7×10^{-9} (e)	1.2×10^{-8} (e)	1.2×10^{-8} (e)	
	Ship/Barge	Atmospheric	2.2×10^{-11} (f)	9.8×10^{-10} (f)	1.3×10^{-9} (f)	
		Pressurized	2.3×10^{-12} (f)	1.6×10^{-11} (f)	3.1×10^{-11} (f)	

Table A5
LOC credit factors for transfer nodes. References for data sources are reported in Table A1.

TRANSFER NODES						
CATEGORY	**SUB-CATEGORY**		**LOC**			**UNITS**
			LOC1	**LOC2**	**LOC3**	
Loading/Unloading hose	Road	Atmospheric	4.0×10^{-6} (a)	7.0×10^{-6} (a) (2)	7.0×10^{-6} (a) (1)	per operation
		Pressurized	4.0×10^{-6} (3)	7.0×10^{-6} (3)	7.0×10^{-6} (3)	
	Rail	Atmospheric	4.0×10^{-6} (a)	7.0×10^{-6} (a) (2)	7.0×10^{-6} (a) (1)	
		Pressurized	4.0×10^{-6} (3)	7.0×10^{-6} (3)	7.0×10^{-6} (3)	
	Ship/Barge	Atmospheric	8.5×10^{-6} (4)	6.3×10^{-5} (4)	6.3×10^{-5} (4)	
		Pressurized	8.5×10^{-6} (4)	6.3×10^{-5} (4)	6.3×10^{-5} (4)	
Loading/Unloading arm	Road	Atmospheric	2.0×10^{-7} (a)	3.2×10^{-6} (a) (2)	3.2×10^{-6} (a) (1)	
		Pressurized	2.0×10^{-7} (3)	3.2×10^{-6} (3)	3.2×10^{-6} (3)	
	Rail	Atmospheric	2.0×10^{-7} (a)	3.2×10^{-6} (a) (2)	3.2×10^{-6} (a) (1)	
		Pressurized	2.0×10^{-7} (3)	3.2×10^{-6} (3)	3.2×10^{-6} (3)	
	Ship/Barge	Atmospheric	3.9×10^{-6} (a)	2.9×10^{-5} (a)	2.9×10^{-5} (a)	
		Pressurized	3.9×10^{-6} (3)	2.9×10^{-5} (3)	2.9×10^{-5} (3)	

(1) obtained from interpolation between two values at 5 and 15 mm.
(2) set equal to LOC3 for lacking further information.
(3) set equal to atmospheric hose/arm for lacking further information.
(4) obtained from leak frequencies of ship arms, using a proportionality factor of 2.

Appendix A. Supporting information

Supplementary data associated with this article can be found in the online version at doi:10.1016/j.psep.2025.108352.

References

Abbate, E., Garmendia Aguirre, I., Bracalente, G., Mancini, L., Tosches, D., Rasmussen, K., Bennett, M.J., Rauscher, H., Sala, S., 2024. Safe Sustain. Des. Chem. Mater. Methodol. Guid. https://doi.org/10.2760/28450.

Ahmad, S.I., Hashim, H., Hassim, M.H., 2014. Numerical Descriptive Inherent Safety Technique (NuDIST) for inherent safety assessment in petrochemical industry. Process Saf. Environ. Prot. 92, 379–389. https://doi.org/10.1016/j.psep.2014.03.009.

Ahmad, S.I., Hashim, H., Hassim, M.H., 2016. A graphical method for assessing inherent safety during research and development phase of process design. J. Loss Prev. Process Ind. 42, 59–69. https://doi.org/10.1016/j.jlp.2015.09.018.

Ahmad, S.I., Hashim, H., Haryani, M., 2017. Inherent Saf. Assess. Tech. Prelim. Des. Stage 56, 1345–1350. https://doi.org/10.3303/CET1756225.

Ahmad, S.I., Hashim, H., Hassim, M.H., Rashid, R., 2019. A graphical inherent safety assessment technique for preliminary design stage. Process Saf. Environ. Prot. 130, 275–287. https://doi.org/10.1016/j.psep.2019.08.024.

AIChE technical manual, 1998. Dow's Chemical Exposure Index Guide. John Wiley & Sons. https://doi.org/10.1002/9780470935309.

Arsad, A.Z., Hannan, M.A., Al-Shetwi, A.Q., Begum, R.A., Hossain, M.J., Ker, P.J., Mahlia, T.I., 2023. Hydrogen electrolyser technologies and their modelling for sustainable energy production: a comprehensive review and suggestions. Int. J. Hydrog. Energy 48, 27841–27871. https://doi.org/10.1016/j.ijhydene.2023.04.014.

Arvidsson, R., Janssen, M., Nordel, A., 2017. Environmental assessment of emerging technologies recommendations for prospective LCA, 22. https://doi.org/10.1111/jiec.12690.

Bassani, A., Vianello, C., Mocellin, P., Angelo, A.D., Spigno, G., Fabiano, B., Maschio, G., Manenti, F., 2023. Aprioristic Integration of Process Operations and Risk Analysis: Definition of the Weighted F & EI-Based Concept and Application to AG2S Technology. https://doi.org/10.1021/acs.iecr.2c02289.

Bergerson, J.A., Brandt, A., Cresko, J., Carbajales-Dale, M., MacLean, H.L., Matthews, H. S., McCoy, S., McManus, M., Miller III, S.A., Posen, W.R.M., Seager, I.D., Skone, T., Sleep, S, T., 2020. Life cycle assessment of emerging technologies: evaluation techniques at different stages of market and technical maturity. J. Ind. Ecol. 11–25. https://doi.org/10.1111/jiec.12954.

Buyle, M., Audenaert, A., Billen, P., Boonen, K., Passel, S.Van, 2020. The Future of Ex-Ante LCA ? Lessons Learned and Practical Recommendations 1–24.

Caldeira, C., Farcal, R., Moretti, C., Mancini, L., Rauscher, H., Rasmussen, K., Riego Sintes, J., Sala, S., 2022b. Safe Sustain. Des. Chem. Mater. Rev. Saf. Sustain. Dimens. Asp. Methods Indic. tools. https://doi.org/10.2760/68587.
Caldeira, C., Farcal, R., Garmendia Aguirre, I., Mancini, L., Tosches, D., Amelio, A., Rasmussen, K., Rauscher, H., Riego Sintes, J., Sala, S., 2022a. Safe Sustain. Des. Chem. Mater. Framew. Défin. Criteria Eval. Proced. Chem. Mater. https://doi.org/10.2760/487955.
Calise, F., Cappiello, F.L., Cimmino, L., D'accadia, M.D., Vicidomini, M., 2021. A review of the state of the art of biomethane production: Recent advancements and integration of renewable energies. Energies 14. https://doi.org/10.3390/en14164895.
Cammann, L., Perera, A., Alstad, V., Jäschke, J., 2024. Design and operational analysis of an alkaline water electrolysis plant powered by wind energy. Int. J. Hydrog. Energy 93, 963–974. https://doi.org/10.1016/j.ijhydene.2024.10.176.
Carvalho, F.S. de, Reis, L.C.B. dos S., Lacava, P.T., Araújo, F.H.M. de, Carvalho, J.A. de, 2023. Substitution of Natural Gas by Biomethane: Operational Aspects in Industrial Equipment. Energies 16. https://doi.org/10.3390/en16020839.
Castellanos-Sánchez, J.E., Aguilar-Aguilar, F.A., Hernández-Altamirano, R., Venegas Venegas, J.A., Raj Aryal, D., 2024. Biogas purification processes: review and prospects. Biofuels 15, 215–227. https://doi.org/10.1080/17597269.2023.2223801.
CCPS, 2019. Guidelines for Inherently Safer Chemical Processes: A Life Cycle Approach, Third Edition. Guidel. Inherently Safer Chem. Process. a Life Cycle Approach, Third Ed. 1–500. https://doi.org/10.1002/9781119529248.
Chau, K., Djire, A., Vaddiraju, S., Khan, F., 2022. Process Risk Index (PRI) – A methodology to analyze the design and operational hazards in the processing facility. Process Saf. Environ. Prot. 165, 623–632. https://doi.org/10.1016/j.psep.2022.07.049.
Cozzani, V., Reniers, G., 2021. Dynamic risk assessment and management of domino effects and cascading events in the process industry. Elsevier B.V, Amsterdam, The Netherlands.
Crivellari, A., Bonvicini, S., Tugnoli, A., Cozzani, V., 2021a. Multi-target Inherent Safety Indices for the Early Design of Offshore Oil&Gas Facilities. Process Saf. Environ. Prot. 148, 256–272. https://doi.org/10.1016/j.psep.2020.10.010.
Crivellari, A., Bonvicini, S., Tugnoli, A., Cozzani, V., 2021b. Key performance indicators for environmental contamination caused by offshore oil spills. Process Saf. Environ. Prot. 153, 60–74. https://doi.org/10.1016/j.psep.2021.06.048.
Cucurachi, S., Giesen, C.Van Der, Guinée, J., 2018. Ex-ante LCA of emerging technologies. Procedia CIRP 69, 463–468. https://doi.org/10.1016/j.procir.2017.11.005.
Delvosalle, C., Fievez, C., Pipart, A., 2004c. APPENDIX 10. Generic Freq. data Crit. Events Aramis Final Use Guide.
Delvosalle, C., Fievez, C., Pipart, A., 2004a. APPENDIX 5. Methodol. Build. Generic Event trees (MIMAH).
Delvosalle, C., Fievez, C., Pipart, A., 2004b. APPENDIX 6. Generic Event trees Gener. MIMAH.
Di Talia, V., Ricci, F., Bonvicini, S., Cozzani, V., 2024. Assessment of Damages to the Environment Due to Natech Accidents: a Case Study. Chem. Eng. Trans. 111, 43–48. https://doi.org/10.3303/CET24111008.
DNV, 2013. Fail. Freq. Guid.
DNV, 2025. PHAST [software] - version 9.11.
Doran, P., Greig, T., 1993. Mond. Index. How Identify Assess. Minimise Potential Hazards Chem. Plant Units N. Exist. Process.
Dumont, E., 2015. H2S removal from biogas using bioreactors: a review. Int. J. Energy Environ. 6, 479–498.
Ee, A.W.L., Kuznetsova, E., Lee, T.E.J., Ng, A.T.S., 2020. Extended inherent safety index -Analysis of chemical, physical and biological inherent safety. J. Clean. Prod. 248, 119258. https://doi.org/10.1016/j.jclepro.2019.119258.
European Commission - JRC, 2010. General guide for Life Cycle Assessment - Detailed guidance, irst editi. ed, Constraints. International Reference Life Cycle Data System (ILCD) Handbook. ublications Office of the European Union, Luxembourg. https://doi.org/10.2788/38479.
Flemish Government, 2009. Handboek Faalfrequenties.
Fossan, I., Opstad, A.S., 2018. Process Leak. Offshore Install. Freq. Assess. Model PLOFAM.
Gangadharan, P., Singh, R., Cheng, F., Lou, H.H., 2013. Novel methodology for inherent safety assessment in the process design stage. Ind. Eng. Chem. Res.
Gao, X., Abdul Raman, A.A., Hizaddin, H.F., Bello, M.M., Buthiyappan, A., 2021. Review on the Inherently Safer Design for chemical processes: Past, present and future. J. Clean. Prod. 305, 127154. https://doi.org/10.1016/j.jclepro.2021.127154.
Gexcon, 2025. EFFECTS [software] - version 12.5.1.
Gkotsis, P., Kougias, P., Mitrakas, M., Zouboulis, A., 2023. Biogas upgrading technologies – Recent advances in membrane-based processes. Int. J. Hydrog. Energy 48, 3965–3993. https://doi.org/10.1016/j.ijhydene.2022.10.228.
Gupta, J.P., Khemani, G., Sam Mannan, M., 2003. Calculation of Fire and Explosion Index (F&EI) value for the Dow Guide taking credit for the loss control measures. J. Loss Prev. Process Ind. 16, 235–241. https://doi.org/10.1016/S0950-4230(03)00044-5.
Heikkil, A., 1999. Inherent Saf. Process Plant Des.
Hendershot, D.C., 1997. Inherently safer chemical process design. J. Loss Prev. Process Ind. 10, 151–157. https://doi.org/10.1016/S0950-4230(96)00055-1.
Hendershot, D.C., 2006. An Overview of Inherently Safer Design. Process Saf. Prog. 25, 326–330. https://doi.org/10.1002/prs.
HSE, 2017. Failure Rate and Event Data for use within Risk Assessments (06/11/17).
IOGP, 2010. Risk Assessment Data Directory - Riser & pipeline release frequencies.
IOGP, 2019a. Risk Assessment Data Directory - Process Release Frequencies.
IOGP, 2019b. Risk Assessment Data Directory - Blowout Frequencies.
IOGP, 2022. Risk Assessment Data Directory - Storage incident frequencies.
ISO, 2016. BS EN 61882:2016 - Hazard and operability studies (HAZOP studies). Application guide.
ISO, 2018. BS ISO 31000:2018 - Standards Publication Risk management — Guidelines, ISO.
ISO, 2020a. BS EN ISO 14040:2006+A1:2020: Environmental management — Life cycle assessment — Principles and framework.
ISO, 2020b. BS EN ISO 14044-2006+A2-2020: Environmental management - Life cycle assessment - Requirements and guidelines.
Janošovský, J., Rosa, I., Vincent, G., Šulgan, B., Variny, M., Labovská, Z., Labovský, J., Jelemenský, Ľ., 2022. Methodology for selection of inherently safer process design alternatives based on safety indices. Process Saf. Environ. Prot. 160, 513–526. https://doi.org/10.1016/j.psep.2022.02.043.
Jiao, W., Xiang, S., 2016. Quantitative Safety and Health Assessment Based on Fuzzy Inference and AHP at Preliminary Design Stage. Iran. J. Chem. Chem. Eng. 35, 153–165.
Kahangamage, U., Chen, K., Zhen, H., Leung, C. wah, 2024. Numerical investigation of combustion characteristics of hydrogen-enriched low calorific value landfill gas for energy applications. Energy Rep. 12, 173–186. https://doi.org/10.1016/j.egyr.2024.06.008.
Khan, F.I., Abbasi, S.A., 1998. Multivariate hazard identification and ranking system. Proc. Saf. Prog. 17, 157–170. https://doi.org/10.1002/prs.680170303.
Khan, F.I., Amyotte, P.R., 2004. Integrated inherent safety index (I2SI): A tool for inherent safety evaluation. Process Saf. Prog. 23, 136–148. https://doi.org/10.1002/prs.10015.
Khan, F.I., Husain, T., Abbasi, S.A., 2001. SAFETY WEIGHTED HAZARD INDEX (SWeHI): A New, User-friendly Tool for Swift yet Comprehensive Hazard Identification and Safety Evaluation in Chemical 79.
Khan, F.I., Sadiq, R., Husain, T., 2002. Risk-based process safety assessment and control measures design for offshore process facilities, 94, 1–36.
Khan, F.I., Sadiq, R., Amyotte, P.R., 2003. Evaluation of available indices for inherently safer design options. Process Saf. Prog. 22, 83–97. https://doi.org/10.1002/prs.680220203.
Kidam, K., Sahak, H.A., Hassim, M.H., Shahlan, S.S., Hurme, M., 2016. Inherently safer design review and their timing during chemical process development and design. J. Loss Prev. Process Ind. 42, 47–58. https://doi.org/10.1016/j.jlp.2015.09.016.
Kletz, T.A., 1996. Inherently safer design: The growth of an idea. Process Saf. Prog. 15, 5–8. https://doi.org/10.1002/prs.680150105.
Kletz, T.A., Amyotte, P., 2010. Process Plants - A Handbook for Inherently Safer Design, 2nd ed. CRC Press, Boca Raton. https://doi.org/10.1201/9781439804568.
Koller, G., Fischer, U., Hungerbu, K., 2000. Assessing Safety, Health, and Environmental Impact Early during Process Development 960–972.
Lawrence, D., 1996. Quantifying inherent Saf. Chem. Process Routes.
Leong, C.T., Shariff, A.M., 2008. Inherent safety index module (ISIM) to assess inherent safety level during preliminary design stage. Process Saf. Environ. Prot. 86, 113–119. https://doi.org/10.1016/j.psep.2007.10.016.
Li, X., Zanwar, A., Jayswal, A., Lou, H.H., Huang, Y., 2011. Incorporating Exergy Analysis and Inherent Safety Analysis for Sustainability Assessment of Biofuels. Ind. Eng. Chem. Res. 50, 2981–2993.
Mannan, S., 2012. Lees' Loss Prevention in the Process Industries. Elsevier. https://doi.org/10.1016/b978-0-12-397189-0.00001-x.
Mansfield, D., J., Clark, Y., Malmén, J., Schabel, R., Rogers, E., Suokas, R., Turney, G., Ellis, J., Van Steen Verwoerd, M., 1997. The INSET Toolkit—Inherent SHE Evaluation Tool.
Norouzi, H., Baradaran, S., Amin, M., 2024. Dev. a Nov. Anticip. Inherent risk Assess. Approach Appl. Early Stages Process Des. Inherent Saf. Assess. Process Equip. 191, 2165–2177.
OREDA, 2002. Offshore Reliability Data Handbook. OREDA, Norw.
Palaniappan, C., Srinivasan, R., Tan, R., 2002a. Expert System for the Design of Inherently Safer Processes. 1. Route Selection Stage 6698–6710.
Palaniappan, C., Srinivasan, R., Tan, R.B., 2002b. Expert System for the Design of Inherently Safer Processes. 2. Flowsheet Development Stage 6711–6722.
Park, S., Xu, S., Rogers, W., Pasman, H., El-Halwagi, M.M., 2020. Incorporating inherent safety during the conceptual process design stage: A literature review. J. Loss Prev. Process Ind. 63, 104040. https://doi.org/10.1016/j.jlp.2019.104040.
Pelucchi, S., Carretta, F., Mocellin, P., Galli, F., 2025. Evaluating process safety at conceptual stage: A stream-based index approach. Process Saf. Environ. Prot. 195, 106830. https://doi.org/10.1016/j.psep.2025.106830.
Pu, W., Abdul Raman, A.A., Hamid, M.D., Gao, X., Buthiyappan, A., 2023. Inherent safety concept based proactive risk reduction strategies: A review. J. Loss Prev. Process Ind. 84, 105133. https://doi.org/10.1016/j.jlp.2023.105133.
Qian, Y., Vaddiraju, S., Khan, F., 2024. Inherent Process Risk Index (IPRI) – A tool for analyzing inherently safer design using Aspen Plus simulation. Process Saf. Environ. Prot. 183, 399–416. https://doi.org/10.1016/j.psep.2023.12.070.
Rahman, M., Heikkilä, A.M., Hurme, M., 2005. Comparison of inherent safety indices in process concept evaluation. J. Loss Prev. Process Ind. 18, 327–334. https://doi.org/10.1016/j.jlp.2005.06.015.
Rathnayaka, S., Khan, F., Amyotte, P., 2014. Risk-based process plant design considering inherent safety. Saf. Sci. 70, 438–464. https://doi.org/10.1016/j.ssci.2014.06.004.
Roy, N., Eljack, F., Jiménez-Gutiérrez, A., Zhang, B., Thiruvenkataswamy, P., El-Halwagi, M., Mannan, M.S., 2016. A review of safety indices for process design. Curr. Opin. Chem. Eng. 14, 42–48. https://doi.org/10.1016/j.coche.2016.07.001.
Rusli, R., Shariff, A.M., Khan, F.I., 2013. Evaluating hazard conflicts using inherently safer design concept. Saf. Sci. 53, 61–72. https://doi.org/10.1016/j.ssci.2012.09.002.

Saccomanno, F.F., Yu, M., Shortreed, J.H., 1993. Risk Uncertainty in the Transport of Hazardous Materials. Transp. Res. Rec. 1383, 58–66.
Sakas, G., Ibáñez-Rioja, A., Ruuskanen, V., Kosonen, A., Ahola, J., Bergmann, O., 2022. Dynamic energy and mass balance model for an industrial alkaline water electrolyzer plant process. Int. J. Hydrog. Energy 47, 4328–4345. https://doi.org/10.1016/j.ijhydene.2021.11.126.
Schlumberger, 2025. OLGA [software] - version 2025.1.0.
Shariff, A.M., Zaini, D., 2010. Toxic release consequence analysis tool (TORCAT) for inherently safer design plant. J. Hazard. Mater. 182, 394–402. https://doi.org/10.1016/j.jhazmat.2010.06.046.
Shariff, A.M., Leong, C.T., Zaini, D., 2012. Using process stream index (PSI) to assess inherent safety level during preliminary design stage. Saf. Sci. 50, 1098–1103. https://doi.org/10.1016/j.ssci.2011.11.015.
Sofu, T., 2015. A review of inherent safety characteristics of metal alloy sodium-cooled fast reactor fuel against postulated accidents. Nucl. Eng. Technol. 47, 227–239. https://doi.org/10.1016/j.net.2015.03.004.
Srinivasan, R., Trong, N., 2008. A statistical approach for evaluating inherent benignness of chemical process routes in early design stages, 86, 163–174. https://doi.org/10.1016/j.psep.2007.10.011.
Tamburini, F., Bonvicini, S., Cozzani, V., 2023. Risk of Subsea Blowouts in Marine CCS. Chem. Eng. Trans. 99, 265–270. https://doi.org/10.3303/CET2399045.
Tamburini, F., Ricci, F., Tzioutzios, D., Paltrinieri, N., 2024b. Understanding Natech Accident Scenarios at Carbon Capture and Storage (CCS) Plants. Chem. Eng. Trans. 111, 391–396. https://doi.org/10.3303/CET24111066.
Tamburini, F., Bonvicini, S., Cozzani, V., 2024a. Consequences of subsea CO2 blowouts in shallow water. Process Saf. Environ. Prot. 183, 203–216. https://doi.org/10.1016/j.psep.2024.01.008.
Tamburini, F., Ricci, F., Cozzani, V., 2025b. Evaluating Natech Risks in the Liquid Hydrogen Maritime Bunkering Infrastructure. Proc. Int. Conf. Offshore Mech. Arct. Eng. OMAE 1, 1–9. https://doi.org/10.1115/OMAE2025-156960.
Tamburini, F., Cozzani, V., Paltrinieri, N., Adams, T.A., 2025a. Weighing risks against GHG reduction benefits in emerging green technologies. Can. J. Chem. Eng. 1–20. https://doi.org/10.1002/cjce.25692.
Thonemann, N., Schulte, A., Maga, D., 2020. How to Conduct Prospective Life Cycle Assessment for Emerging Technologies ? A Systematic Review and Methodological Guidance 1–23.
TNO, 2005. Guidelines for quantitative risk assessment (purple book). Publ. Ser. Danger. Subst.
Tugnoli, A., Cozzani, V., Landucci, G., 2007. A consequence based approach to the quantitative assessment of inherent safety. AIChE J. 53, 3171–3182. https://doi.org/10.1002/aic.11315.
Tüysüz, H., 2023. Alkaline Water Electrolysis for Green Hydrogen Production. Acc. Chem. Res. https://doi.org/10.1021/acs.accounts.3c00709.
US EPA, 2024. ALOHA [software] - version 5.4.7.
Wang, W., Liang, K., Wang, C., Wang, Q., 2014. Comparative analysis of failure probability for ethylene cracking furnace tube using Monte Carlo and API RBI technology. Eng. Fail. Anal. 45, 278–282. https://doi.org/10.1016/j.engfailanal.2014.06.024.
Warnasooriya, S., Gunasekera, M.Y., 2016. Assessing inherent environmental, health and safety hazards in chemical process route selection. Process Saf. Environ. Prot. 105, 224–236. https://doi.org/10.1016/j.psep.2016.11.010.
Zanobetti, F., Tugnoli, A., Cozzani, V., 2023. Challenges to ISD application. Methods Chem. Process Saf. 214–244.
Zanobetti, F., Pozzo, A.D., Cozzani, V., 2025. Sustainability assessment of CO2 capture across different scales of hard-to-abate emission sources. Chem. Eng. J. 505, 159466. https://doi.org/10.1016/j.cej.2025.159466.